Shades of White: Impacts of Population Dynamics and TV Viewership on Available TV Spectrum

Zhongyuan Zhao, *Member, IEEE*, Mehmet C. Vuran, *Member, IEEE*, Demet Batur, and Eylem Ekici, *Fellow, IEEE*

***Abstract*—Current regulations leave a few television (TV) white spaces in populated urban areas where spectrum shortage is mostly experienced. As TV set feedback becomes essential in the next generation terrestrial TV standard, an opportunistic TV spectrum sharing based on TV receiver activity information and transmit power control is proposed to exploit the underutilized active TV channels. Based on investigation of the spatial–spectral–temporal characteristics of TV receiver activities, analytical models are developed to capture the spatio-temporal distributions of available spectrum and corresponding capacity. The influence of multiple factors, such as feedback delay, spectrum handover overhead, ranking order, and distribution of TV channel popularity are discussed and modeled. The proposed power control mechanism is verified through experiments at representative campus and residential environments. Empirical data-based simulations and geographic analyses are conducted to evaluate the developed models and further profile the spectrum opportunities within a cell, across New York city (NYC) and other 273 cities in the United States. In NYC, the proposed solution provides a 3.8–11.7-fold increase of average spectrum availability, and 2.5–6.6-fold increase of capacity from current regulations. By investigating the feasibility and prospects of this approach, this paper intends to motivate further discussions in policy, business, and privacy aspects to reach its significant potential.**

***Index Terms*—TV white space, black space, cognitive radio networks, dynamic spectrum access, TV ratings.**

I. Introduction

TO ADDRESS the emerging *spectrum crisis* [1], unlicensed Television Band Devices (TVBDs) are allowed to operate in TV white spaces (TVWS) in the U.S. under regulations set forth by the Federal Communications Committee (FCC) [2], [3]. TVWS, defined as geographical areas where over-the-air (OTA) TV services are unavailable [2], is accessed primarily via relatively static spectrum databases. By keeping interference from *potential* TV users, this approach, however, left populated urban areas, where spectrum shortage is most severe, with too few TVWS [4]–[6]. For example, 4 out of the 5 largest cities by population, which are also of the top-8 cities by GDP (New York, Los Angeles, Chicago, Philadelphia), have less than 4 TVWS channels for portable TVBDs. The lack of economy of scale due to poor penetration in urban markets is a significant roadblock for TVWS technology [7].

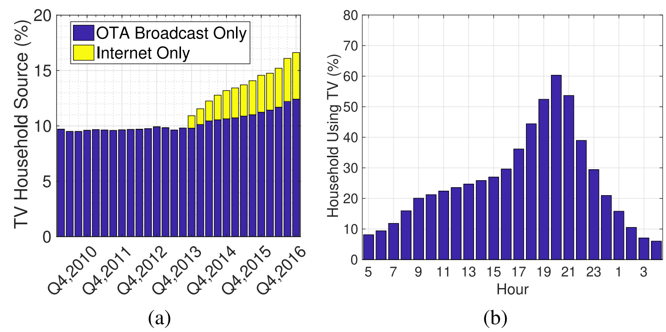

Fig. 1. TV Usage in the U.S. (a) TV Usage By Source, 2010–2016 [10]. (b) 24-hour TV Usage Pattern [11]–[13] (pp. 323).

The economic-based initiatives of the FCC, such as imposing spectrum fees, encouraging channel sharing, and enabling incentive auctions of the spectrum, however, face strong opposition from incumbent licensees [8]. It is until 2017 FCC re-purposed 70 MHz spectrum in its first broadcast incentive auction and the transition periods will last to 2020 [9]. The timeliness and effectiveness of these approaches are still unclear given increased TV users chosen broadcast-only TV recently (Fig. 1(a)). Further progress on the urban spectrum crisis yet relies on the advances in coexisting technologies.

From the perspective of TV viewers, even active TV channels are underutilized. By 2016, only 13.3% of the U.S. TV households solely use OTA broadcast services [10]. The percentage of households using television, fluctuates from 7.6% during the midnight to 60% during prime time (Fig. 1(b)) [11]–[13], with only a few TV channels being watched at a time in a household. Spatially, underutilization also occurs in where OTA TV households are absent [14].

The biggest challenge of systematically utilizing active TV channel is acquiring the activity of TV receivers. Recent proposals, such as gray space (TVGS) in Norway [14], low power coexistence by Ofcom [15], and cellular TV distribution [16], avoid involving TV users due to the difficulty of TV receiver

Manuscript received May 21, 2018; revised October 18, 2018; accepted December 11, 2018. Date of publication January 14, 2019; date of current version March 14, 2019. This work was supported by NSF under Grants CNS-1247941 and CNS-1247914. This paper was presented in part at the IEEE Global Communications Conference, Austin, TX, USA, December 2014. The review of this paper was coordinated by Prof. W. A. Krzymien. *(Corresponding author: Zhongyuan Zhao.)*

Z. Zhao and M. C. Vuran are with the Department of Computer Science and Engineering, University of Nebraska-Lincoln, Lincoln, NE 68588 USA (e-mail: zhzhao@cse.unl.edu; mcvuran@cse.unl.edu).

D. Batur is with the Department of Management, University of Nebraska-Lincoln, Lincoln, NE 68588 USA (e-mail: dbatur@unl.edu).

E. Ekici is with the Department of Electrical and Computer Engineering, The Ohio State University, Columbus, OH 43210 USA (e-mail: ekici@ece.osu.edu).

This paper has supplementary downloadable material available at http://ieeexplore.ieee.org, provided by the author.

Digital Object Identifier 10.1109/TVT.2019.2892867

detection [17]. However, TV set will not be a passive receiver forever. In fact, inspired by the emerging Internet TV (Fig. 1(a)), the next generation TV standard, Advanced Television Systems Committee (ATSC) 3.0 [18], approved by FCC in 2017 [19], will replace current one-way terrestrial TV system with a Hybrid broadcast broadband Television system featured with TV set feedback, to enable fully interactive [20] and personalized TV program.

Therefore, TV viewer-facilitated unlicensed spectrum access is not only feasible but also desirable: it resolves the conflict of interests between an ubiquitous broadband [21] and TV industry by giving incumbent licensees business opportunities to serve unlicensed users, meanwhile opening more urban markets to TVBD.

Unlike previous TVWS papers assuming non-cooperative TV sets, in this paper, we systematically investigate the feasibility and prospects of TV spectrum sharing facilitated by cooperative TV viewers. Specifically, a technical framework, Cognitive Television (Cog-TV), is proposed as the potential next generation TV set capable of providing Wireless Local Area Network (WLAN) or small cell services to residential and commercial places with restricted footprint. Based on investigation of TV usage and traffic pattern, analytical models are developed for the availability, capacity, and characteristics of the spectrum enabled by this framework. The impacts of signaling latency and spectrum handover overhead on both primary and secondary users are analyzed. Through experiments and empirical data-based simulation and geographical analysis, we validate the proposed framework and models, characterize the spectrum opportunities in geographical, spectral, and temporal dimensions, and profile its potential on national scale. Findings of this paper shed light on the potential service quality, enhancements and restrictions of the TV viewer-facilitated spectrum access. Hopefully, it would motivate more discussions in technology, business, and policy aspects.

The rest of this paper is organized as follows: Related works are reviewed in Section II. The Cog-TV framework is introduced in Section III. In Section IV, TV network is characterized and spectrum availability is modeled. Power control and achievable capacity are modeled in Section V. Evaluations on cellular, city, and national scales are presented in Sections VI, VII, and VIII, respectively. The paper is concluded in Section IX with a discussion on future directions.

II. Related Work

A. TV Spectrum Availability

The spectrum availability and Shannon capacity of TVWS by geography and population in the continental US [4], [22] and Europe [23] are quantitatively analyzed based on TV station registration information and radio propagation models.

These well-established methodologies, as summarized in [5], lay the foundations of current database-driven TVWS technology [24], [25], and are employed in this paper to estimate the contours and signal strength of TV services.

Propagation model-based approaches, due to the precision of propagation models, predict limited TVWS in urban areas, where abundant TVWS caused by shadowing and/or penetration loss of buildings has been identified by measurement campaigns [26]–[31], especially indoors [31]–[33]. To exploit such TVWS, measurement-based enhancements, e.g. large spectrum sensor network [31], [32] and radio environment map [34], are proposed. But the gains could be offset by efforts of improving OTA TV signal penetration, e.g. single frequency network [18]. More importantly, existing works on TVWS focus mainly on the characteristics of primary *transmitters* while ignoring the primary *receivers*.

Secondary spectrum access in legacy TV service area (TV black-space (TVBS)) is a recently evolving topic [14], [33], [35]–[40]. In [14], [36], guard zone of TVWS is applied on TV receivers to protect them from co-channel secondary users (SUs). A static map of spectrum availability (gray space) is obtained with registered addresses and channel subscriptions of TV receivers [14]. But this approach is limited to mandatory TV receiver registration and low population density.[1] SUs in gray-space also face the strong interference of primary signal [39]. In [36], a secondary WiFi testbed, using a smart remote for TV receiver feedback, achieved a capacity of 20 Mbps on an active TV channel by mitigating interference from and to SU via beamforming and interference cancellation (IC), respectively. The feasibility of accessing active TV channel on physical layer is demonstrated in [36]. Instead of using guard zone associated with fixed SU transmit power, our work further restricts SU footprint via transmit power control, and puts emphasis on network layer to analyze the feasibility and prospect of TV receiver-assisted spectrum access *at scale*. Protection of PUs in TVBS is further supported by an analytical model of aggregate interference from heterogeneous, interweaving SUs to primary receivers [40].

In [37], a theoretical model of available spectrum and capacity is developed based on the statistics of TV channel usage, for scenarios in which SUs use identical transmit power, and all TV channels are from a single TV tower. In contrast, our models capture dynamic SU transmit power, and realistic settings of multiple TV towers. The relevant concepts of spatio-spectral space in TV spectrum sharing are summarized in Table I. Gray space is already included in TVBS, thus no longer discussed separately. To the best of our knowledge, our work is the first theoretical modeling and empirical data-based analysis of the spatial-spectral-temporal dynamics of spectrum availability and capacity on TVBS for cellular to city-wide scales.

B. Dynamic Spectrum Access

Cog-TV network accesses TV spectrum as a SU and shall not interfere with primary users (PUs) (active TV viewers). Under such a hierarchical dynamic spectrum access (DSA) model, spectrum sharing approaches for SUs include underlay, overlay, interweave, and their combinations [41]. In this paper, a combination of underlay and interweave DSA is considered: Within

[1] With 16 dBm Effective Radiated Power (ERP) limit, 13.3% OTA TV ownership rate (Section VII-A), and guard zone of 910 m [14] (Smaller for indoors [33]), gray space requires a population density $\leq 8.7/\text{km}^2$ [38], which is far below the average density in 274 major US cities (Fig. 19(b)).

TABLE I
CONCEPTS OF SPATIO-SPECTRAL SPACE IN TV SPECTRUM SHARING

White Space (TVWS)	TV service is inactive or shadowed; always accessible to qualified SU[2].
Gray Space (TVGS)	TV service is active, TV receiver is absent; always accessible to qualified SU.
Black Space (TVBS)	TV service is active; accessible to qualified SU, when TV receivers are absent or inactive.

[2] Qualified SU refers to meeting requirements, such as transmit power, antenna, geolocation capability according to rules.

a given area, SUs exploit the spectrum holes through spectrum management functionality [1], [42], meanwhile limit their transmit power to avoid harmful interference to PU receivers outside that area [41].

Alternatively, overlay-based spectrum access is developed to enhance the TV viewer experience via rebroadcasting the TV signal while hiding the secondary signal in it [43]. However, it requires external TV content feeds at SU transmitter which is difficult for portable TVBDs. Nevertheless, its TV signal cancellation technique could enhance SU receiver performance.

C. Primary Receiver Sensing

Leveraging TV receiver activity requires the knowledge of locations and spectrum occupations of nearby TV receivers. One approach is to detect TV receiver via the local oscillator (LO) leakage power emitted by the RF front-end [44]. Detecting the weak LO leakage at longer distances is difficult [17], but collaborative spectrum sensing could be employed to exploit multi-dimensional correlation (spatial, temporal, and spectral) for better accuracy and complexity [45].

Another approach to obtain TV viewer activity is to attach additional devices to TV receivers. Existing examples include the Nielsen TV meters installed in roughly 10,000 US households for collecting TV usage activities [46], and smart remote for spectrum management in [36]. Locations of TV receivers could be obtained by incentivizing a voluntarily registration [14], or requiring geo-location capability [2]. Existing technical [36] and business cases [46] set valuable examples for the scalability of this approach in practice.

The most thorough approach is to embrace the next generation terrestrial TV standard, ATSC 3.0, where TV receiver feedback via broadband or dedicated return channel becomes a standard feature in order to provide interactive and personalized TV services [18], [19]. This Internet Protocol (IP)-based new standard is designed to replace current OTA TV system without backward compatibility. Therefore, obtaining real-time channel occupation information of TV receivers in large scale may no longer be difficult. Moreover, this spectrum sharing mode engages TV networks in a more sustainable way than existing spectrum auction and leasing [9], [47]. However, further discussions w.r.t. policy and privacy, and relevant designs of protocol and infrastructure are required.

III. COG-TV FRAMEWORK

A. Spectrum Access

The spectrum access under Cog-TV framework is illustrated by an exemplary scenario (Fig. 2(a)) with three OTA TV services (channels 23, 27, and 45), multiple active TV receivers, and two SU links. The channels viewed by PUs are indicated by the number above. Zones c_1 and c_2 are the regions where SU links c_1 and c_2 will interfere co-channel PUs, respectively. Based on FCC rules, link c_1 can access all the three channels, as none of them are served in zone c_1; while link c_2 can access none of these channels, since they are all served in zone c_2. However, under Cog-TV framework, channel 45 is available for link c_2 for it is not used by any PU in zone c_2.

B. Reference Network Architecture and Cellular Structure

Consider the reference network architecture in Fig. 2(b), which contains a primary network composed of TV towers and receivers, and a co-existing secondary network (Cog-TV network) composed of secondary access points (SU APs) and user equipments (SU UEs). SU APs are connected to the Internet via backhaul or fronthaul. A Cog-TV device integrates SU AP and TV set, and can be a new TV model or a Set-Top-Box (STB) connected to a traditional TV set.

When using OTA TV services, Cog-TV device would register its ID and address, and keep updating its TV channel selections. A list of TV channels available to the SUs is maintained in real-time based on the local TVWS retrieved from spectrum databases, and locations and channel usage of OTA TV receivers in the interference zone of an SU AP (discussed next). The SU AP schedules the spectrum access of attached UEs, evacuates TV channels for arriving PUs, and may cooperate with neighboring SU APs for frequency reuse and mobility management.

The combination of underlay and interweave DSA employed to access TVBS, is represented by a Cog-TV cell (Fig. 2(c)). The service zone of SU AP has a radius of d, which is the maximum distance between SU AP and SU UE for sufficient performance. TV signal at SU receiver is either ignored as noise [4] or mitigated by interference cancellation (IC) [43], [48]. The region with radius R is called the *interference zone*. SUs employ transmit power control, as detailed in Section V, to avoid interference to any co-channel PU receivers beyond a distance R from SU AP. SUs only access TV channels not being viewed by any PU in the interference zone. Multiple access in Cog-TV cell is assumed to be collision-free.

C. TV Spectrum Concepts and Regulation

Cog-TV framework is built on concepts in TVWS regulations. Currently, TV spectrum is shared to SU on the basis of analog TV channel of unit bandwidth, W_0, e.g. 6 MHz in the US, 8 MHz in Europe. Of the entire TV spectrum ($\{[2, 69]\backslash 37\}$ in the US), only a subset is open for DSA, referred as TVWS band ($\{[2, 51]\backslash\{3, 4, 37\}\}$ in the US [2]). Restrictions on power, antenna height, and frequency are differentiated by the type of TVBD [2]. In the US, fixed TVBD can access the entire TVWS band, while portable TVBD can only access an UHF subset, $\{[21, 51]\backslash 37\}$, referred as portable TVWS band [2]. Four sets of channels are considered in a specific geographical area: *OTA service set*, denoted as $\mathbb{T}$, refers to all active TV channels in TV spectrum. *TVWS set*, denoted as $\mathbb{W}$, refers to all white-space channels under established regulation, e.g. FCC rules [2]. *Reserved set*, denoted as $\mathbb{E}$, refers to all channels excluded from

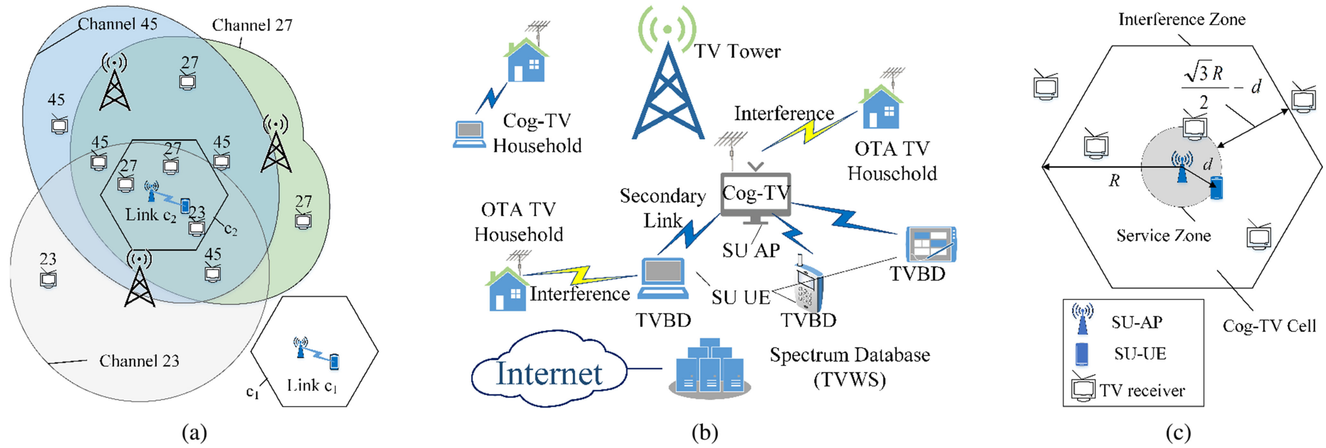

Fig. 2. Cog-TV framework. (a) Cog-TV Spectrum Access. (b) Reference Network Architecture. (c) Cellular Structure.

SU for other regional services, e.g. PLMRS/CMRS. *TVBS set*, denoted as $\mathbb{B}$, refers to all active, unreserved channels in TVWS band, and $\mathbb{B} \in \mathbb{T} \setminus \{\mathbb{W} \cup \mathbb{E}\}$.

IV. Black Space Spectrum Availability

Spectrum availability (SA) refers to the number of TV channels available to SU.

In relatively static TV spectrum sharing [5], [14], [22], [23], SA is a time-invariant function of geo-location with an integer value for each location. For TVBS that is accessible to SU opportunistically, SA is defined as the *expected* number of available TV channels, and could be a fraction. In this section, TVBS SA on cellular level is firstly modeled, then the spectral and spatial characteristics of PUs, as well as practical concerns in network and market penetration are investigated. Then, we model the TVBS SA in a city, followed by the variation of rating ranking.

A. Black Space Spectrum Availability

Consider a Cog-TV cell c is covered by an OTA service set, $\mathbb{T}_c = \{b_1, \ldots, b_j, \ldots, b_{|\mathbb{T}_c|}\}$, and each TV receiver (PU) in cell c is independently tuned to a channel in $\mathbb{T}_c$ at a time or turned off.

Identical distribution of channel holding time on all the channels is assumed, due to its weak correlation with channel popularity [49]. PU traffic is assumed to follow a Poisson arrival process in a short time interval (e.g. 15 minutes) based on empirical measurements of live IPTV system [50], [51]. Since unlimited TV receivers can simultaneously access an OTA TV channel, TV channel $b_j \in \mathbb{T}_c$ is modeled as a $M/G/\infty$ queue, where the PU is the customer with Poisson arrivals at rate $\lambda_c(b_j, t)$, and the channel holding time of PU, denoted as B, is the service time modeled as a random process following a general distribution. PU access of OTA service set in cell c is modeled as a network of $M/G/\infty$ queues connected in parallel, as shown in Fig. 3. With Poisson arrivals, each $M/G/\infty$ queue operates independently [52, Ch. 3.2].

Accordingly, n_j, the number of PUs being tuned to TV channel b_j in cell c, follows a Poisson distribution. The idle proba-

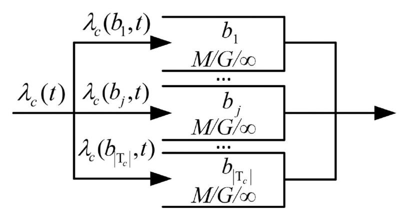

Fig. 3. Queueing Network Model of Spectrum Access for Primary Users (TV Viewers) in a Cog-TV Cell.

bility of channel b_j (no PU in cell c on channel b_j) is:

$$Pr\{n_j = 0\} = e^{-\lambda_c(b_j,t)E(B)}, \tag{1}$$

where $E(B)$ is the average channel holding time. In the $M/G/\infty$ queueing system, the average number of customers being served is $E(n_j) = \lambda_c(b_j,t)E(B)$, and the idle periods have an exponential length with mean $[E(n_j)]^{-1}$. On the spatial dimension, since TV receivers are mostly fixed household appliances, the spatial distribution of PU is modeled as a Poisson Point Process (PPP) [53] with density, $\lambda(c)$, at cell c. Thus, $E(n_j)$ can also be estimated by

$$E(n_j) = \lambda_c(b_j,t)E(B) = \lambda(c)\mathbb{A}(c)\alpha_c(b_j,t), \tag{2}$$

where $\mathbb{A}(.)$ is the function of area, $\mathbb{A}(c)$ denotes the area of cell c, and $\alpha_c(b_j,t)$ is the rating of channel b_j at time t. Note that this queueing network is quasi-stationary [50] due to the varying activity of TV viewers as discussed in Section IV-B. Therefore, time t is included in the model.

Based on the spectrum access in Section III-A, a TVBS channel $b_j \in \mathbb{B}_c$ is available to SU in its idle periods. The availability of TVBS channel b_j is a Bernoulli random variable (R.V.), of which the mean is defined as the SA of b_j, denoted as $\delta_j(c,t)$, and is equal to the probability for SU to access b_j. With (1) and (2), the SA of a channel b_j is:

$$\delta_j(c,t) = \mathbb{I}(b_j \in \mathbb{B}_c)\, e^{-\lambda(c)\mathbb{A}(c)\alpha_c(b_j,t)}, \tag{3}$$

where $\mathbb{I}(.)$ is indicator function, and $\mathbb{B}_c$ is the TVBS set at cell c. Note that (1), (2), and (3) indicate that SA, $\delta_j(c,t)$, depends on rating over a period rather than that of a moment.

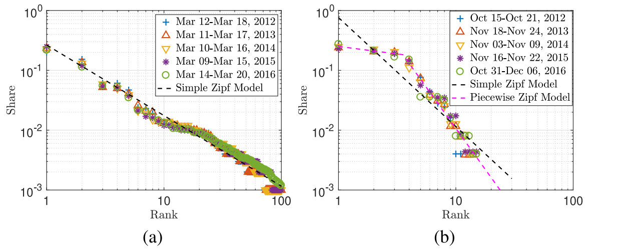

Fig. 4. Weekly TV Viewer Shares 2012-2016. (a) Top-100 TV Channels in UK [56]. (b) OTA TV Networks [57] During Prime Time in the US[2].

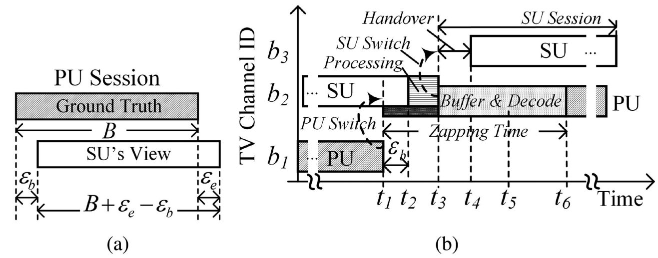

Fig. 5. Impacts of Signaling and Handover Latency. (a) TV Receiver Feedback Delay. (b) An Exemplary Spectrum Handover.

The number of available TVBS channels in cell c at any moment is the sum of independent Bernoulli R.Vs. with different success probabilities, which follows a Poisson Binomial distribution [54].

The TVBS SA is the mean of the Poisson Binomial distribution:

$$\Delta(c,t) = \sum_{b_j \in \mathbb{B}_c} \delta_j(c,t) = \sum_{b_j \in \mathbb{B}_c} e^{-\lambda(c)\mathbb{A}(c)\alpha_c(b_j,t)} . \quad (4)$$

Local TVBS set $\mathbb{B}_c$ can be estimated by approaches in [4], [5]. The rating of channel b_j, $\alpha_c(b_j,t)$, and TV receiver density, $\lambda(c)$, are discussed in Sections IV-B and IV-C, respectively.

B. TV Rating Model

TV rating is the percentage of the universe of TV viewers tuned to a TV channel at the same time [55]. National and regional TV ratings [56], [57], estimated from a sufficiently large set of TV household samples [46], are commercially available and served as currency of TV industry. According to Law of Large Numbers, the probability of a TV receiver tuned to a TV channel is equal to its rating.

The rating of channel $b_j \in \mathbb{T}$ at time t, $\alpha(b_j,t)$, is:

$$\alpha(b_j,t) = \varphi(t) r(b_j) , \quad (5)$$

where $\varphi(t)$ is Households Using Television (HUT), $r(b_j)$ is the viewer share of channel b_j [55].

HUT is the percentage of TV households in a geographical area with at least one TV set in use during a specific period [55]. The pattern of HUT in a day (Fig. 1(b)) is repeatable [58]–[60], and is modeled as a function of time t, and assumed to be stationary and consistent regionally. The viewer share (SHR) of a channel is the percentage of active TV receivers tuned to that channel simultaneously [55]. SHR represents channel popularity, and is normalized over $\mathbb{T}$ by definition. If a city y is partially covered by some channels in $\mathbb{T}_y$, SHR of a TV channel b_j in a cell, $r_c(b_j)$, may not be equal to that in the city, $r_y(b_j)$, as $\mathbb{T}_c \subseteq \mathbb{T}_y$.

IPTV studies [58]–[61] show that SHR follows Zipf distribution: SHR of a TV channel can be predicted by its rank of popularity [61]. This is also found in the weekly SHRs of top-100 channels in UK [56] (Fig. 4(a)) and top-15 OTA networks in the US (Fig. 4(b)) from 2012 to 2016. For generality, we model SHR as a K-piecewise Zipf distribution [38](Section III).

Zipf-distributed SHR implies that most TV viewers watch a few very popular channels, leaving SUs more opportunities. For comparison, *random* and *uniform*-distributed SHR [35] are also considered. Random SHR is generated as an uniformly-distributed random vector with lower peak-to-average ratio than Zipf SHR, representing moderate scenarios when few popular programs are aired. Uniform SHR, where all channels are viewed at equal chance, serves as worst case analysis of the lower bound of TVBS SA, although it rarely occurs.

SHR exhibits geographical locality due to local TV networks and geographical variation of the OTA service set [58]. SHR of top-rated channel in IPTV system can vary up to 20% across country [58]. Regional SHR can predict SA with better accuracy than national SHR, but is costly and less accessible. The impact of SHR variation is evaluated in Section VII-C.

C. TV Receiver Location

Television is highly popular in residential and commercial places, e.g., 99% households in the US have TV sets, with mean 2.93 sets per household [62]. Thus, it is reasonable to assume that TV receivers are co-located with population. TV receiver density $\lambda(c)$ in a cell c, is modeled as:

$$\lambda(c) = \rho(c)\eta(c) \quad (6a)$$

$$\approx \rho(c)\eta , \text{ for } \eta \approx \eta(c) , \forall c , \quad (6b)$$

where $\rho(c)$ is the population density at cell c, and $\eta(c)$ is the OTA TV ownership rate (number of OTA TV receivers over population) at cell c. The approximation in (6) is found by replacing local OTA TV ownership rate $\eta(c)$ with a more available national OTA TV ownership rate η. Potential spatial bias of this approximation, e.g. $\eta(c)$ in central business district may be much lower than rural areas without cable TV, would underestimate SA in urban areas.

D. Network Imperfection

A Cog-TV receiver informs SU network whenever it starts or ends a session. SU is notified after a random delay due to network and processing latency [63]. The length of PU session perceived by SU is $B + \varepsilon_e - \varepsilon_b$, where ε_b and ε_e are random signaling delays in the beginning and end of actual PU session, respectively (Fig. 5(a)), and follow identical distributions due to common underlying processes. As a result,

[2]US ratings are only partially available. Weeks are picked as close as possible to eliminate seasonality, which could be captured by separated estimates. Unpicked weeks are used to validate the model in Section VII-C. (set as footnote)

$E(B+\varepsilon_e-\varepsilon_b)=E(B)$. Based on Section IV-A, SA of a TVBS channel is determined by the average PU session length, $E(B)$. Moreover, TV receivers could never interfere SU. Therefore, in theory, TVBS SA is not influenced by network and processing latency. We show this in Section VI-A via simulations and in [63] via experiments.

Next, we consider a PU-triggered spectrum handover (Fig. 5(b)). At t_1, PU initiates a switch from channel b_1 to b_2, which is being used by an SU link. Due to signaling latency, the SU link is informed at t_2, and switches from channel b_2 to a free channel b_3 at t_3. The SU link starts communication at t_4 when connectivity on channel b_3 is established. PU begins receiving TV signal on channel b_2 at t_3 when SU is evacuated. After a period of buffering and decoding [64], the first frame of image is displayed on PU screen at t_6. Without the SU link, however, PU could start receiving on channel b_2 at t_1 and display image earlier at $t_5=t_6-t_3$.

For TV viewers, the degradation of quality of experience (QoE) due to SU manifests as longer zapping time [64], e.g. t_6-t_1 instead of t_5-t_1 in Fig. 5(b).

Typical zapping time of digital TV receiver is 1–2 sec [64], and an acceptable increase, e.g, $5\%\sim30\%$, allows an evacuation time of 0.1–0.3 sec for SU, which is feasible with off-the-shelf technologies, i.e. round-trip latency of 12–58 ms for US broadband during peak traffic [65], slot length of 10-20 ms for WiFi and LTE networks, and radio cutting off time of 0.1 ms, e.g. in LTE-TDD.

For SU, the effective SA depends on lengths of SU session and spectrum handover, as analyzed in Section VI-A.

E. Market Penetration

TVBS could be accessed by SU when Cog-TV feature of all the TV sets in a Cog-TV cell are activated. Suppose the activation in a market proceed gradually under the supervision of network operator, and define penetration rate, η_m, as the number of Cog-TV device over all TV sets, then the enabling probability of a Cog-TV cell c, denoted as $\theta(c)$, is:

$$\theta(c)=e^{-\lambda(c)\mathbb{A}(c)(1-\eta_m)}\ . \tag{7}$$

We analyze this in [38].

F. Distribution of Black Space Spectrum Availability

Consider a city y is defined by its contour, S_y, the set of all OTA TV channels in city y is $\mathbb{T}_y$, and the coverage area of a TV channel b_j is defined by its contour, $S_{t,j}$. If $S_y\not\subset S_{t,j}$, then in a part of the city, $S_{b,j}=S_y\cap S_{t,j}$, channel b_j is a TVBS channel, $(S_{b,j}\neq\emptyset\ ,\forall b_j\in\mathbb{T}_y)$, whereas in the remaining, $S_{w,j}=S_y\setminus S_{t,j}$, it is a white space channel.

1) Homogeneous Coverage: Consider a city y' is fully covered by all the TV channels in $\mathbb{T}_{y'}$, $(S_{b,j}=S_{y'},\forall b_j\in\mathbb{T}_{y'})$, and the SHR of a TV channel b_j is $r_{y'}(b_j)$. Based on (3), (5) and (6), the CDF of SA on a TVBS channel b_j in the city y', at time t is

$$F_{\delta,b_j,y',t}(x)=Pr\left\{\theta(c)\delta_j(c,t)\leq x|c\in S_{y'}\right\} \tag{8a}$$

$$\approx Pr\left\{e^{-\rho(c)\eta\mathbb{A}(c)\left[r_{y'}(b_j)\varphi(t)+1-\eta_m\right]}\leq x|c\in S_{y'}\right\}\ , \tag{8b}$$

Based on (4), the CDF of SA of TVBS set across city y' at time t is

$$F_{\Delta,y',t}(x)=Pr\left\{\theta(c)\Delta(c,t)\leq x|c\in S_{y'}\right\} \tag{9a}$$

$$\approx Pr\left\{\sum_{b_j\in\mathbb{B}_{y'}}e^{-\rho(c)\eta\mathbb{A}(c)\left[r_{y'}(b_j)\varphi(t)+1-\eta_m\right]}\leq x|c\in S_{y'}\right\}. \tag{9b}$$

2) General Case: For a city y with heterogeneous TV coverage, $(S_{b,j}\neq S_y,\exists b_j\in\mathbb{T}_y)$, we divide city y into a set of sub-regions, $\{y_m,|\ m=1,\ldots,2^{|\mathbb{T}_y|}\}$. The contour of y_m is:

$$S_{y_m}=S_y\cap\bigcap_{b_j\in\mathbb{T}_{y_m}}S_{b,j}\setminus\bigcup_{b_i\in\mathbb{T}_y\setminus\mathbb{T}_{y_m}}S_{b,i}\ ,\mathbb{T}_{y_m}\in\mathbb{P}(\mathbb{T}_y)\ , \tag{10}$$

where $\mathbb{P}(\mathbb{T}_y)$ is the power set of $\mathbb{T}_y$. By (10), for $S_{y_m}\neq\emptyset$, sub-region y_m is fully covered by all channels in $\mathbb{T}_{y_m}$. Based on (8), the CDF of SA on a TVBS channel b_j in city y at time t is:

$$F_{\delta,b_j,y,t}(x)=\sum_{m=1}^{2^{|\mathbb{T}_y|}}\vartheta_{y_m}F_{\delta,b_j,y_m,t}(x)\ , \tag{11}$$

where ϑ_{y_m} is the ratio of the area of sub-region y_m and city y, $\mathbb{A}(S_y)=\vartheta_{y_m}\mathbb{A}(S_{y_m})$. Based on (9), the CDF of SA of TVBS set across city y at time t is:

$$F_{\Delta,y,t}(x)=\sum_{m=1}^{2^{|\mathbb{T}_y|}}\vartheta_{y_m}F_{\Delta,y_m,t}(x)\ . \tag{12}$$

Since $\mathbb{T}_{y_m}\subseteq\mathbb{T}_y$, the SHR of channel $b_j\in\mathbb{T}_{y_m}$, $r_{y_m}(b_j)$ need to be adjusted according to the SHR rank of b_j within $\mathbb{T}_{y_m}$:

$$r_{y_m}(b_j)=Z(k_{y_m}(b_j))\left[\sum_{i=1}^{|\mathbb{T}_{y_m}|}Z(i)\right]^{-1}\ , \tag{13}$$

where $Z(.)$ is defined in (1) in [38], and $k_{y_m}(b_j)$ is the rank of b_j in $\mathbb{T}_{y_m}$:

$$k_{y_m}(b_j)=\sum_{b_i\in\mathbb{T}_{y_m}}\mathbb{I}(k(b_i)<k(b_j))\ , \tag{14}$$

where $\mathbb{I}(.)$ is the indicator function.

Accordingly, the average TVBS SA of a channel b_j across the city y, at time t is

$$E(\delta_j(c,t)\mid c\in y)=\int_0^1 xf_{\delta,b_j,y,t}(x)\mathrm{d}x\ , \tag{15}$$

where $f_{\delta,b_j,y,t}(x)$ is the PDF of SA of TVBS channel, b_j. Based on (15), the average total TVBS SA at time t across city y is:

$$E(\Delta(c,t)\mid c\in y)=\sum_{b_j\in\mathbb{B}_y}E(\delta_j(c,t)\mid c\in y)\ , \tag{16}$$

G. Temporal Variations in TV Channel Popularity

Despite relatively stationary SHRs of TV networks, as discussed in Section IV-B, mapping from TV networks to OTA service set for each market (e.g. city) in the US is unique and dynamic. To capture the uncertainty introduced by such dynamics, we model the variation of TVBS SA with randomly ranked OTA TV channels. At time t, $\Delta(c,t)$ in (4), and $E(\Delta(c,t) \mid c \in y)$ in (16) are functions of rank vector $\mathbf{k}$ with following form:

$$V_{\Delta,t}(\mathbf{k}) = \sum_{b_j \in \mathbb{T}} \mathbb{I}(b_j \in \mathbb{B}) U(k(b_j)) \,, \tag{17}$$

where if $V_{\Delta,t}(\mathbf{k})$ stands for $\Delta(c,t)$ for cell c, then $U(k(b_j))$ refers to (3); if $V_{\Delta,z,t}(\mathbf{k})$ stands for $E(\Delta(c,t) \mid c \in y)$ for city y, then $U(k(b_j))$ refers to (15). $U(k(b_j))$ is obtained by plugging (5), (1) in [38], (13), and (14) into (3) or (15). Since $\mathbf{k}$ is a random permutation of $\langle 1, \ldots, |\mathbb{T}| \rangle$ (Supplemental material [38] (Section III)), if $\mathbb{B} \neq \mathbb{T}$, $V_{\Delta,t}(\mathbf{k})$ follows a Normal distribution given in supplemental material [38] (Section IV) based on Combinatorial Central Limit Theorem [66]. This model is validated in Section VII-C. Since $U(.)$ in (17) is monotonically increasing, the lower bound of $V_{\Delta,t}(\mathbf{k})$ can be obtained by a special rank vector with the most popular channels in $\mathbb{B}$, $\mathbf{k}_L \in \{\mathbf{k} \mid k(b_j) < k(b_i), \forall b_j \in \mathbb{B}, \forall b_i \in \mathbb{T} \setminus \mathbb{B}\}$.

V. Achievable Capacity

The achievable capacity of Cog-TV on the edge of service zone is modeled based on the SA model and Shannon capacity (w/ distance of d). For the latter, radio propagation, TV towers, and SU power control are considered. The model is based on a single antenna, and could be further extended to capture MIMO, full duplex radio, and protocol overheads.

A. Cellular Capacity

The achievable capacity in a Cog-TV cell c at time t is $C(c,t) = C^b(c,t) + C^w(c)$, where $C^w(c)$ and $C^b(c,t)$ are the capacities of local TVWS and TVBS sets, respectively. The total capacity of local TVBS set is the sum of session capacities weighted by SA of all TVBS channels:

$$C^b(c,t) = W_0 \sum_{b_j \in \mathbb{B}_c} \delta_j(c,t) \log(1+\psi_j) \,, \tag{18}$$

where ψ_j is the SINR on channel b_j at SU receiver given by

$$\psi_j = \frac{P_j L_j^s h G_t G_r}{N_0 W_0 + I_j^{s2s} + I_j^{p2s}} \,, \tag{19}$$

where P_j is the SU transmit power, L_j^s is the path loss from SU transmitter to SU receiver, modeled as a function of distance $L(.)$, h is the fading coefficient, N_0 is thermal noise floor, I_j^{s2s} and I_j^{p2s} are interferences from SUs outside cell c, and TV towers of the same & adjacent channels, respectively. G_t and G_r are gains of transmit and receive antennas, respectively.

Local TVWS set is considered always available to SUs on the scale of minutes to days, thus its total capacity is:

$$C^w(c) = W_0 \sum_{b_j \in \mathbb{W}_c} \log(1+\psi_j) \,, \tag{20}$$

In TVWS, SU adopts established transmit power limits, e.g. 16 dBm ERP, which already protects PUs on adjacent channels [5]. The I_j^{p2s} is mainly from adjacent channel TV towers and/or distant co-channel ones. In contrast, I_j^{p2s} in TVBS is dominated by TV signals from co-channel towers, which by regulation is much stronger (e.g. ≥ 23 dB) than undesired TV signals from adjacent channels [15], [67], [68], therefore the latter could be ignored. Next, transmit power control to restrict the footprint of SU in TVBS is introduced.

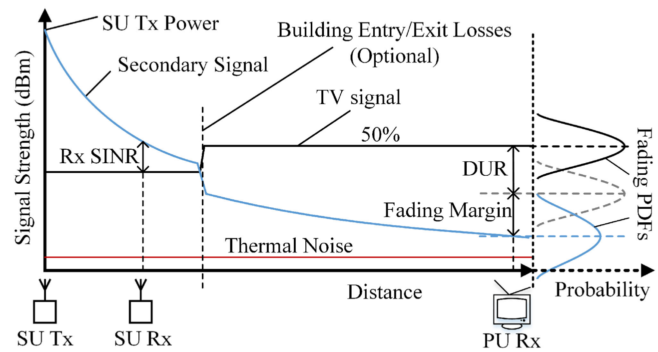

Fig. 6. Cog-TV Power Control Scheme with Path Loss Model.

B. Power Control

Consider the propagation of TV and secondary signals on a TVBS channel in a Cog-TV cell, as illustrated in Fig. 6. The average outdoor TV signal strength in a Cog-TV cell is approximately constant, since TV towers are usually far from the city, variation of the path loss experienced by TV signal in a few hundred meters is negligible. The secondary signal at a SU receiver within distance of service radius d, is much less attenuated than that at a co-channel PU receiver beyond interference radius R, for R would be many-times greater than d. SU transmit power is adjusted accordingly so that secondary signal is sufficiently attenuated at R.

Regulators require that a minimum Desired to Undesired signal Ratio (DUR) at PU receiver [15], [67] shall be guaranteed with a high probability [69], as expressed in dB-domain:

$$Pr\left\{\mathbf{dB}(\zeta_j'(c)) - \mathbf{dB}(\beta) \geq \mathbf{dB}(I_j^{s2p})\right\} = H_{Th} \,, \tag{21}$$

where $\mathbf{dB}(.) = 10\log_{10}(.)$ represents dB-domain, β and H_{Th} are the required minimum DUR and protection probability, respectively, and $\zeta_j'(c)$ is the TV signal strength in cell c. Additionally, regulators set maximum transmit power limit to SU [5], denoted as P^{max}.

Based on (21), we define R.V. $\omega = \mathbf{dB}(\zeta_j'(c)) - \mathbf{dB}(\beta) - \mathbf{dB}(I_j^{s2p})$. Consider a propagation with log-normal fading, the SU-to-PU interference, I_j^{s2p}, and the TV signal strength, $\zeta_j'(c)$, at PU receiver, both follow log-normal distributions: $\mathbf{dB}(I_j^{s2p}) \sim \mathrm{N}(\mathbf{dB}(P_j L_j^{s2p}), \sigma_s)$, and $\mathbf{dB}(\zeta_j'(c)) \sim \mathrm{N}(\mathbf{dB}(\zeta_j(c)), \sigma_b)$, where L_j^{s2p} is the SU-to-PU path loss, σ_s and σ_b are the dB-domain standard deviations of fading in short-distance and broadcast propagation models, respectively, and $\zeta_j(c)$ is the dB-domain mean TV signal strength on channel b_j in cell c. Since secondary and TV signals experience fading independently, R.V. ω, as the difference of two independent, normally distributed R.Vs., also follows a Normal distribution [70]:

$$\omega \sim \mathrm{N}\left(\mu_\omega, \sigma_\omega\right) \ , \tag{22a}$$

$$\text{where, } \mu_\omega = \mathbf{dB}\big(\zeta_j(c)\big) - \mathbf{dB}(\beta) - \mathbf{dB}(P_j L_j^{s2p}), \tag{22b}$$

$$\sigma_\omega = \sqrt{\sigma_s^2 + \sigma_b^2} \ . \tag{22c}$$

Based on (21) and (22), there is

$$Q\left(\frac{-\mu_\omega}{\sigma_\omega}\right) = H_{Th} \ . \tag{23}$$

With (22), (23), and transmit power limit P^{max}, the transmit power for SU is determined by:

$$P_j = \max\left(\frac{\zeta_j(c)}{\gamma\beta L_j^{s2p}}, P^{max}\right) , \tag{24}$$

where γ is the fading margin, defined as:

$$\mathbf{dB}(\gamma) = \mu_\omega = -Q^{-1}(H_{Th})\sqrt{\sigma_s^2 + \sigma_b^2} \ . \tag{25}$$

To ensure any co-channel PU receivers are protected with probability $\geq H_{Th}$, $L_j'^{s2p} = L_j\left(\sqrt{3}R/2 - d\right)$, the worst-case SU-to-PU path loss, is used in (24), where $\sqrt{3}R/2 - d$ is the shortest distance between co-channel SU and PU (Fig. 2(c)).

It can be observed from (24) that under certain network configurations and radio propagation environment, SU transmit power, P_j, increases with TV signal strength, but will be limited to $P_j = P^{max}$ when TV signal is too strong, $\zeta_j(c) \geq \zeta_j^T$, where the threshold $\zeta_j^T = P^{max}\gamma\beta L_j'^{s2p}$.

C. Distribution of Achievable Capacity in Black Space

To model the distribution of achievable TVBS capacity in a city y, we consider a random cell $c \in S_y$, of which all location-related properties are also R.Vs. For convenience, we use R.Vs. C_t^b, $C_{j,t}^b$, $\delta_{j,t}$, and ζ_j to represent the total TVBS capacity, $C^b(c,t)$, TVBS capacity on channel b_j, $C_j^b(c,t)$, SA, $\delta_j(c,t)$, and TV signal strength, $\zeta_j(c)$, respectively, of the random cell c. In city y, $F_{\delta,b_j,y,t}(x)$, the CDF of SA on a TVBS channel b_j, is given in (11), and $F_{\zeta_j,y}(x)$, the CDF of TV signal strength on channel b_j, can be obtained through geographical analysis [5].

Since the TV signal strength in neighboring cells are similar, the SU transmit power in neighboring Cog-TV cells is also similar according to (24). Therefore, it is safe to assume identical P_j across neighboring cells. Based on (19) and (24), the SINR of a SU receiver at the distance of service radius, denoted as ψ_d, is a function of ζ_j:

$$\psi_d(\zeta_j) = \frac{P_j L_j^s}{N_0 W_0 + P_j L_j^{s2s} + \zeta_j v} \tag{26a}$$

$$\begin{cases} \approx \frac{L_j^s}{v\gamma\beta L_j'^{s2p} + L_j^{s2s}}, & \zeta_j < \zeta_j^T \\ = \frac{P^{max} L_j^s}{N_0 W_0 + P^{max} L_j^{s2s} + v\zeta_j}, & \zeta_j \geq \zeta_j^T \end{cases} , \tag{26b}$$

where L_j^s is the path loss of the secondary link, L_j^{s2s} is the path loss of the SU to SU interference, and the approximation in (26) is by ignoring $N_0 W_0 / P_j$.

Based on Shannon capacity, the session capacity on a TVBS channel b_j with distance d is a function of TV signal strength, ζ_j:

$$C_j^* = g(\zeta_j) = W_0 \log_2\big(1 + \psi_d(\zeta_j)\big) \ . \tag{27}$$

For $\zeta_j < \zeta_j^T$, the maximum session capacity is:

$$C_{j,max}^* = W_0 \log_2\left(1 + \frac{L_j^s}{L_j^{s2s} + v\gamma\beta L_j'^{s2p}}\right) \ . \tag{28}$$

Based on (26) and (27), the inverse function of $g(.)$ is:

$$\zeta_j = g^{-1}(C_j^*) = \frac{1}{v}\left(\frac{P^{max} L_j^s}{2^{C_j^*/W_0} - 1} - P^{max} L_j^{s2s} - N_0 W_0\right) \ . \tag{29}$$

According to (26), ψ_d is a constant when $\zeta_j < \zeta_j^T$, and is a monotonic decreasing function of ζ_j when $\zeta_j \geq \zeta_j^T$. Therefore, the CDF of session capacity on channel $b_j \in \mathbb{B}$ is:

$$F_{C_j^*,y}(x) = \begin{cases} 1 - F_{\zeta_j,y}\big(g^{-1}(x)\big), & x < C_{j,max}^* \\ 1, & x = C_{j,max}^* \end{cases} . \tag{30}$$

Achievable capacity of a channel $b_j \in \mathbb{B}_y$ is the product of SA and session capacity, $C_{j,t}^b = \delta_{j,t} C_j^*$. Assuming $\delta_{j,t}$ and C_j^* are independent from each other, the PDF of achievable capacity on channel b_j is [71]:

$$f_{C_{j,t}^b,y}(x) = \int_0^1 f_{\delta,b_j,y,t}(w) f_{C_j^*,y}\left(\frac{x}{w}\right) \mathrm{d}w \ , \tag{31}$$

where $f_{\delta,b_j,y,t}(x)$ and $f_{C_j^*,y}(x)$ are PDFs of SA and session capacity on channel b_j, respectively. Based on (31), the CDF of achievable capacity on TVBS channel b_j is:

$$F_{C_{j,t}^b,y}(x) = \int_0^\infty f_{C_{j,t}^b,y}(x)\mathrm{d}x + F_{\delta,b_j,y,t}(0) \ . \tag{32}$$

Finally, the average achievable capacity of TVBS channel b_j, and of TVBS set, $\mathbb{B}_y$, in city y are:

$$E\Big(C_j^b(c,t) \mid c \in y\Big) = \int_0^\infty x f_{C_{j,t}^b,y}(x)\mathrm{d}x \ , \tag{33}$$

$$E\Big(C^b(c,t) \mid c \in y\Big) = \sum_{b_j \in \mathbb{B}} E\Big(C_j^b(c,t) \mid c \in y\Big) \ , \tag{34}$$

respectively. Validations of these models are presented in Section VII and VIII.

VI. Cellular Model Evaluation

The cellular SA model and transmit power control are the major components in modeling SA and capacity. The former is evaluated numerically with empirical TV user traffic in Section VI-A, and the latter is verified through measurement campaigns in Section VI-B. City-wide and national evaluations are presented in Sections VII and VIII, respectively. A cell size of $R = 150$ m is used for all evaluations based on numerical searching for maximum capacity across cities [38].

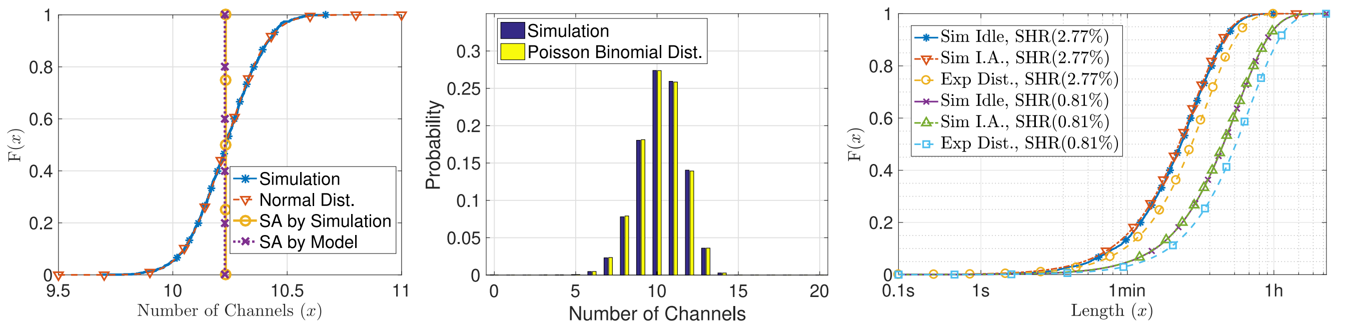

(a) Spectrum Availability (b) Instantaneous Channels (c) Idle Period Length Distribution

Fig. 7. Characteristics of Black-Space Spectrum Availability from Simulation with length of 30 days and 1000 replications.

A. Spectrum Availability

1) Simulation Setup: A hexagonal Cog-TV cell (Fig. 2(c)) is configured for a scenario of portable TVBD band with reserved channels in New York City (NYC). The OTA service set has 51 channels, of which the SHRs are generated by a 2-piecewise Zipf model (Fig. 4(b)) [57] ($\tau_1 = 0.2517$, $\tau_2 = 2.7312$, $a_1 = 0.2513$, $a_2 = 5.7637$). 20 top-rated channels with a total SHR of 62.2% are observed. In the simulation, virtual TV receivers are generated as a PPP with a density from (6) based on peak Zip code population density of 58,000/km^2 in NYC [72], a HUT of 60% (Fig. 1(b)) [12], and OTA ownership rate of 13.3%, which is based on $14,706,000$ OTA TV households [10], population of $323,148,587$ [73] in 2016, and 2.93 sets per TV household [62]. This worst-case setting emulates the busiest PU traffic in real-world. TV receiver behavior is generated by a mixed exponential distribution (MED) model that captures surfing, viewing, and away [74]. Each TV receiver is randomly initialized based on MED model, and tuned to a channel with the probability of its SHR in each channel session. Note that since HUT in MED model is fixed to 41.66%, OTA TV ownership rate is adjusted to 19% for equal traffic volume. The MED model is based on empirical data of over 2 million STBs of a live IPTV system in the US [74]. IPTV offer similar user experiences as OTA TV system, for which there is no publicly available measurements with similar scale and granularity. The MED model is representative of OTA TV users. It can test the accuracy of our model under an empirical traffic without Poisson arrivals [74]. Finally, the simulation time is 30 days, with 1,000 replications.

2) Simulation Results: In each replication, SA of an observed channel is collected as the total idle time over simulation time, and the TVBS SA as sum of SA of the 20 channels. The CDF of TVBS SA of 1,000 replications fits well with a Normal distribution with mean of 10.227, and standard deviation of 0.474 (Fig. 7(a)), which is consistent with Central Limit Theorem. The empirical mean TVBS SA is only 0.05% less than theoretical value of 10.232. Similar accuracy is obtained with other population density, SHR [56], and traffics [50], [51], [58].

The number of instantaneously available channels is sampled every 6 minutes, of which the PMF (Fig. 7(b)), is consistent with corresponding Poisson Binomial distribution, despite the fact that the arrival process is non-Poisson. Moreover, the probability of 5+ channels being available at any moment is 99.93%, suggesting that a very reliable network connectivity could be supported in a realistic setting.

The length of idle periods on each channel is also collected. The top-5 channels by popularity w/ SHRs from 6.94% to 24.56% are unavailable in the simulation. Only the 6th (SHR $= 2.77\%$) and 7th (SHR $= 0.81\%$) most popular channels are presented in Fig. 7(c) due to space limits. The CDFs of simulated idle period length (Sim Idle), are closer to that of the inter-arrival time of TV users (Sim I.A.), than to the exponential idle periods length from queueing model (Exp Dist.) as shown in Fig. 7(c). The median idle period length predicted by model is 43% longer than that of the non-Poisson empirical PU traffic. Rest of the channels have similar results. Therefore, our model can characterize the length of TVBS spectrum holes with sufficient accuracy.

Compared to typical OFDM slot, e.g. 20.46 ms in 802.11n, 10 ms in LTE-A, most spectrum holes on TVBS are orders of magnitude longer, e.g. on the 6th (7th) most popular channel, 98.1% (99.45%), and 84.3% (95.22%) of idle periods are longer than 10 sec, and 1 minutes, respectively. This result is representative of the rest of the channels as lower SHR lead to longer idle periods, and Zipf SHR predicts low SHRs on most channels. Therefore, overhead of spectrum handover, e.g. a mean of 130 ms in Cog-TV prototype [63], is insignificant, if not negligible.

B. Transmit Power Control Site Survey

Protection of co-channel PU under transmit power control is evaluated by an experiment emulating Cog-TV network operated in representative business and residential environments.

1) Experimental Setup: In the experiment, an SU transmitter (Tx) transmits a test OFDM signal on TVWS channels, and a receiver (Rx) measures the receive signal strength (RSS) of TV and test signals. The Tx is implemented with an USRP B200 [75] and a dipole antenna with center frequency of 433 MHz and gain of 5.5 dBi. The Rx is implemented with a spectrum analyzer (N9912A) and a wide-band (30–3000 MHz) omni-directional antenna, and has a sensitivity of -93 dBm at 6 MHz. The Tx and Rx devices are shown in Fig. 8. Measurement campaigns are conducted on a campus site (Fig. 9(a)) and a residential site (Fig. 9(b)). The Tx is placed on the indoor ground floor at locations of red triangles. Locations of Rx are marked by blue squares, where SU Rx and PU Rx on cell edge are labeled by

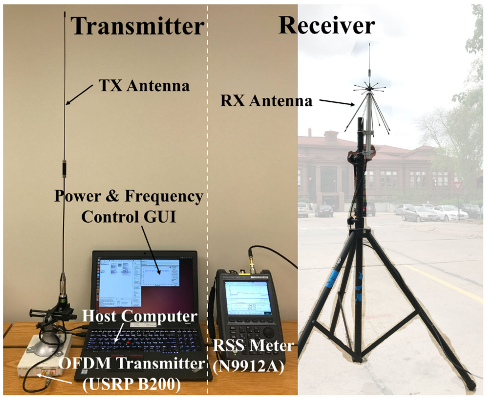

Fig. 8. Transmitter and Receiver Devices for Site Survey.

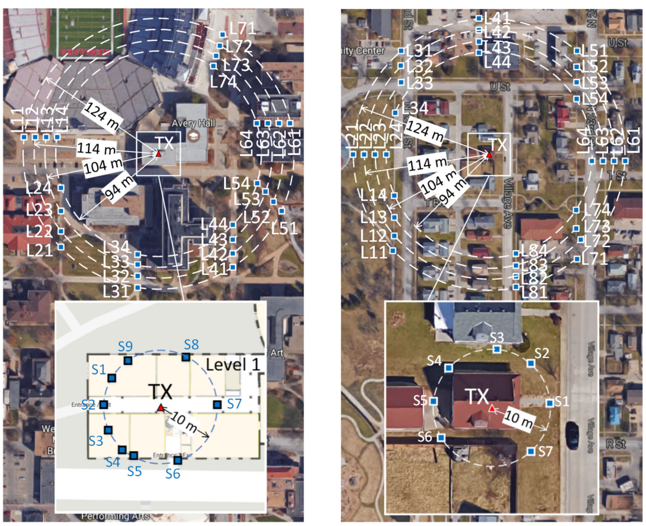

(a) Campus Site (b) Residential Site

Fig. 9. Locations of Transmitter and Receivers in Site Survey.

TABLE II
MEASUREMENT CONFIGURATIONS IN SITE SURVEY

Tx Antenna Height	1.5 m above the floor, 3 m (campus) and 2.5 m (residential) above street levels.
Rx Antenna Height	1.5 m at SU Rx locations, 3 m at TV receiver (PU) locations
Test OFDM Signal	5.5MHz bandwidth, power 13.5 dBm, BPSK modulation, random bits as payload
Test Channels	Black-Space: $\{22, 26, 31, 43, 45\}$, White Space $\{21, 23, 25, 27, 30, 33, 42, 44, 45\}$

S and L, respectively. The distance of 94–124 m between Tx and PU Rx is selected based on Rx sensitivity and cell size. Configurations of antenna heights, test OFDM signal, and test TV channels, are listed in Table II.

In compliance with TVWS regulations, test signal is transmitted on TVWS channels, $b_j \pm 1$, that sandwich a TVBS channel b_j. Since propagation characteristics on nearby frequencies are similar, the attenuation of test signal on TVBS channel b_j is approximated by measurements on channels $b_j \pm 1$. Tx is off while measuring the RSS of TV signal on channel b_j.

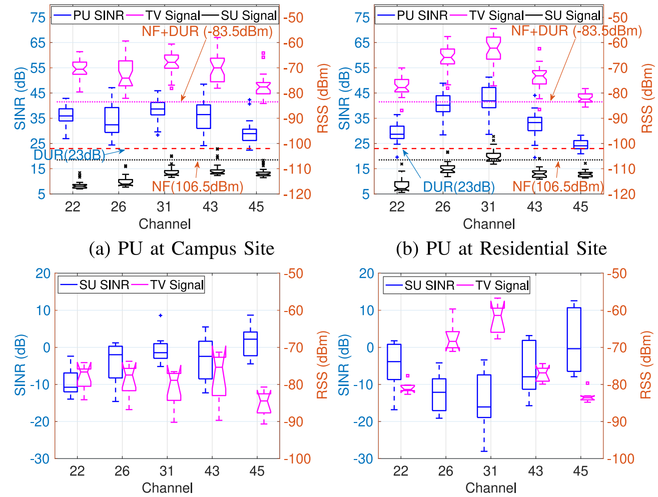

(a) PU at Campus Site (b) PU at Residential Site

(c) SU at Campus Site (d) SU at Residential Site

Fig. 10. Measured SINR of SU and PU at Campus and Residential Sites.

The intended SU transmit power on a TVBS channel is calculated based on (24) with following inputs: $\zeta_j(c)$ and σ_b are the mean and standard deviation in decibel of TV RSS measured at all outdoor Rx locations ($\sigma_b = 4.74$ dB and 4.81 dB on campus and residential sites, respectively), $\beta = 23$ dB, $\sigma_s = 7.02$ [76], and pathloss, L_j^{s2p}, is based on ITU-R P1411 [76] with a distance of 114 m. Then, the difference between intended and actual transmit power is added to the measured RSS as calibrated RSS with power control. Finally, SINRs at SU and PU receivers with power control are calculated for each channel-location sample. The calibrated test OFDM signal and TV signal are signal and interference for SU, respectively, and vise versa for PU.

2) Experiment Results: The SINR, RSSs of TV and SU signals (with power control) at PU receivers on campus and residential sites are presented in Figs. 10(a) and 10(b), respectively. Most channel-location samples have good TV signal (23 dB or more above thermal noise floor (NF)), only 1.43% (campus) and 7.5% (residential) are weak (worst: -86.9 dBm). SU signal at PU receivers ranges from -119 to -97 dBm, mostly below NF. With power control, PU SINR are all above the required DUR of 23 dB except those samples with weak TV signal. Those exceptions could be eliminated with typical TV antenna with gain of 6–20 dBi. This results show that co-channel TV receivers with location uncertainty of ± 20 m are protected by SU power control.

The SINR and TV RSS at SU receiver with power control on campus and residential sites are presented in Figs. 10(c) and 10(d), respectively. On campus site, SU SINR (all indoors) varies from -14.6 and 8.7 dB with a mean of -3.1 dB. On residential site, SU SINR (all outdoors) varies from -28.1 to 12.6 dB with a mean of -7.2 dB. The observed inverse correlation between SU SINR and TV RSS shows that SU performance is dominated by TV RSS. Thus, SU reception could be further improved by TV signal cancellation. Comparison of indoor and outdoor SU receivers inside another building 55–68 m from SU Tx shows that shielding of buildings benefit indoor SU by attenuating interference from both TV stations and neighboring

SUs [38]. Power control with site-specific propagation model can further improve SU SINR [38].

VII. City Wide Evaluation

Next, we evaluate the spatio-temporal dynamics and distributions of spectrum availability (SA) and capacity in representative urban (NYC) and rural (Lincoln, Nebraska) cities, based on real-world data of population and TV stations. The prime-time results are presented in Sections VII-B–VII-C (SA), and Section VII-D (capacity), and the temporal dynamics of SA are in Section VII-E.

A. Evaluation Setup

The city is divided into hexagonal grids (cells), and models are validated via three approaches:

- **Simulation:** Virtual TV receivers are generated according to a PPP in a city based on OTA TV receiver density map. For each instance, a snapshot of channel selections of all the TV receivers is randomly generated based on local OTA service set and ratings, and unused TV channels in each cell are counted as available. 1,000 instances are simulated.
- **Micro model:** The SA of each cell in a city is estimated by cellular analytical models in (4), based on local OTA TV receiver density, OTA service set, and ratings.
- **Macro model:** The CDFs of SA and achievable capacity in a city are estimated by city-level analytical models in (9), and (32) and (34), respectively, based on TV ownership and viewership data, and distributions of population density and TV signal strength.

For the first two approaches, capacity estimation is based on (19) and (32). The runtime of a simulation instance and macro model is similar to and only 5% of micro model, respectively.

The signal strength and contours of TV services are from [4], [5] based on a spectrum database [24] with PLMRS/CMRS channels reserved. The density map of TV receivers is based on OTA TV ownership rate of 13.3%, HUT of 60% [12], and Zip code population density from CENSUS 2010 [72], where density within a Zip code is assumed to be uniform as a trade off between accuracy and complexity. For SHRs, Zipf model in Section VI-A, random and uniform models [35] are evaluated. To be conservative, a random rank vector per city is generated by constraints of $\mathbf{k}_L$ in Section IV-G. TV and SU networks are configured as a household scenario, with parameters of transmit power, antenna, cellular dimensions listed in Table III. Unless otherwise noted, the default setting is urban indoor w/o IC, and wall penetration losses are from [67].

For a fair comparison between Cog-TV and TVWS (FCC rules) in an WLAN setting, 16dBm ERP limit is applied to fixed TVBD on all TV channels, to allow its operation on TVWS channel adjacent to TVBS channel. Since the restricted footprint of Cog-TV could allow flexible rules for other users, e.g. wireless microphone, restrictions on channels 36, 38 and channels dedicated to wireless microphone are relaxed as earlier TVWS works did [4], [5], [23]. As a result, our results for TVWS may show 1-2 more channels than spectrum databases [24].

TABLE III
Network Configurations for City-Wide Evaluation

Item	TV Network	Secondary Network
BS Antenna Height	Specified in [25]	3m (below rooftop)
User Antenna Height	10m above rooftop	1.5m above ground
Antenna Directivity	Isotropic	Isotropic
Emission Power	Specified in [25]	by power control
Propagation Model	F-curves [77]	Urban: ITU-R P1411 [76], Suburban: TM91 [67], [78]
Service Contour & Footprint	Contours from [25] RSS by Calculation	Cell in Fig. 2(c), $d = 10, 20\text{m}$, $R = 150\text{m}$
MISC.	DUR = -23 dB, $H_{Th} = 90\%$ [69]	Interference Mitigation $v = -20dB$ [43], [48]

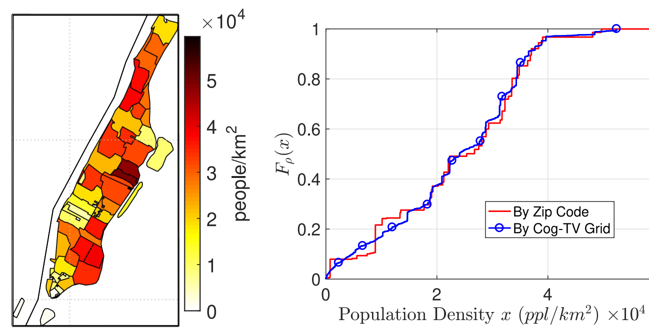

(a) Heat Map (b) CDFs

Fig. 11. Zip Code Population Density in New York City [72].

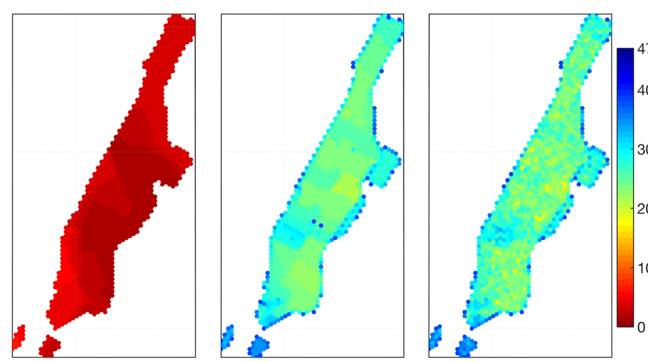

(a) (b) (c)

Fig. 12. Heat Maps for SA in TVWS band in NYC with Zipf SHRs. (a) FCC rule. (b) Theoretical Cog-TV SA from Micro Model. (c) Snapshot Cog-TV SA, An Simulation Instance.

B. Spectrum Availability

In a city with abundant TV services, such as NYC, SA under FCC rules (TVWS) is limited and homogeneous (Fig. 12(a)) as it depends on TV service contours. In contrast, SA under Cog-TV framework (Fig. 12(b)) is significantly increased by additional TVBS SA. TVBS SA depends on the activity and locations of TV receivers, thus is correlated with population density (Fig. 11(1)), and more spatially heterogeneous and dynamic than TVWS. SA under Cog-TV has stochastic nature as shown in a snapshot from simulation (Fig. 12(c)), which has randomness across cells and is consistent with theoretical SA (Fig. 12(b)) from *micro model* at Zip code.

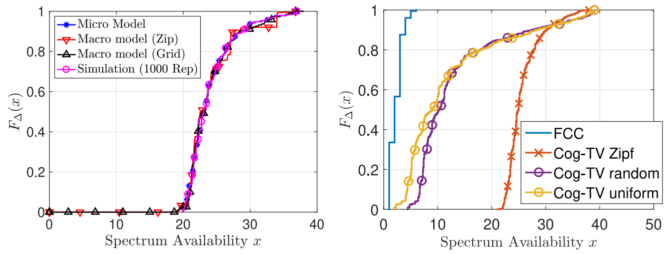

(a) (b)

Fig. 13. CDFs of Spectrum Availability in NYC from different approaches. (a) Blace-Space SA with Zipf SHRs from Multiple Approaches. (b) SA of TVWS and Cog-TV with Zipf, Random, and Uniform SHRs.

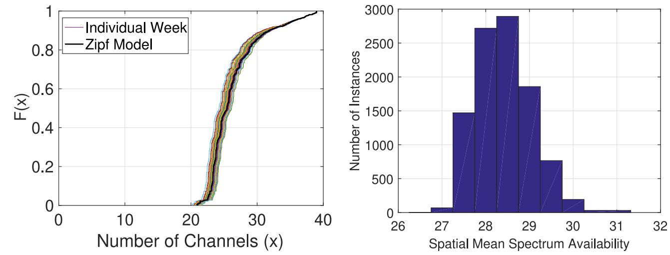

(a) (b)

Fig. 14. SA in NYC under Temporal Variations in Ratings. (a) CDFs of Cog-TV SA based on Zipf SHR, and 46 individual weekly SHRs from 2011 to 2016. (b) Histogram of City-Wide Average SA from 10000 Instances of Random Rank Vector.

TABLE IV
AVERAGE NUMBER OF CHANNELS IN PRIME TIME

Rules	Rating	NYC (total 38)		Lincoln (total 47)	
		Fixed	Portable	Fixed	Portable
FCC	-	2.26	1.36	28.92	18.19
Cog-TV	Zipf	26.41	18.52	45.94	29.73
	Random	11.83	8.15	45.74	29.17
	Uniform	8.50	6.06	45.71	29.18

Two CDFs of SA are estimated by macro model based on the CDFs of population density in NYC at granularities of Zip code and grid (Fig. 11(b)), respectively, where the CDF by grid is smoothened by grids across multiple Zip codes. Compared to the CDF of SA from *simulation*, RMS of CDFs of SA from *micro model*, and *macro model* with Zip code and grid level inputs (Fig. 13(a)) are 0.3%, 2.4%, and 1.3%, respectively. It shows that the cellular SA model is more accurate than city-wide model, and finer granularity of population density yields better accuracy.

SA of TVBS is significantly influenced by distribution of SHRs. The CDFs of SA in NYC with Zipf, random, and uniform SHRs (Fig. 13(b)) show that as channel popularity becomes more equal, TVBS SA becomes more dynamic (standard deviation from 3.6, to 7.9, and 9.2). The average SA of NYC and Lincoln under FCC rules and Cog-TV framework is reported in Table IV. Random and uniform SHRs only have 53% and 43% of average SA as Zipf SHR for fixed TVBD band in NYC, respectively. However, influence of SHR distribution vanishes as the density of active TV receivers approaches 0. The average SA in Lincoln varies only 0.5% with different SHRs.

In NYC, Cog-TV could introduce a 3.8–11.7-fold increase of SA over TVWS for fixed TVBDs, and a 4.5–13.6-fold increase for portable TVBDs. As shown in [38], average SA in NYC is 22.7 even for a OTA TV ownership of 38% (Including viewers of OTA TV programs via cable, satellite, and Internet). In Lincoln, Cog-TV could make nearly all the TVWS band (98.4% of fixed TVBD band and 98.7% of portable TVBD band on average) available for SUs.

C. Impact of Temporal Variations in Ratings

The CDFs of Cog-TV SA obtained by *macro model* based on 2-piecewise Zipf SHRs, and 46 individual weekly SHRs[3]

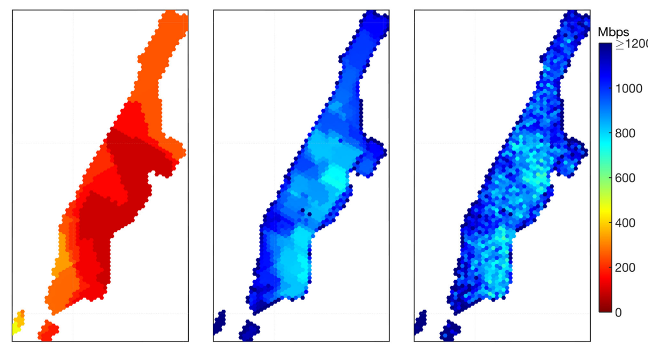

(a) (b) (c)

Fig. 15. Indoor Achievable Capacity in NYC, Fixed TVBD band, Zipf Rating, $d = 10$ m, ITU-R P1411, Capacity $\geq$ 1.2 Gbps in Dark blue. Heat maps. (a) TVWS. (b) TVWS+TVBS. (c) TVWS+TVBS w/ Fading.

(excluding the 5 weeks in Fig. 4(b)) from 2011 to 2016, are compared in Fig. 14(a). The individual CDFs of 46 weeks are very close to the CDF from Zipf model, with a standard deviation of 0.35 for the means of the 46 weeks. It suggests that Cog-TV SA with Zipf SHR is insensitive to temporal fluctuation or geographical locality for top-rated channels.

With the 2-piecewise Zipf SHR, Cog-TV SA in NYC is evaluated with 10,000 random rank vectors. NYC is fully covered by 35 of 42 OTA TV channels (38 TVBS), and the coverage ratio of other 7 channels ranges from 70.7% to 99.8%. The city-wide average SA from those rank vectors follows a Normal distribution (Fig. 14(a)) as predicted in Section IV-F with a standard deviation of 0.56. It shows that SA from a random SHR rank vector is representative, especially as the OTA TV coverage in most US cities exhibit high degree of homogeneity [6].

D. Achievable Capacity

In NYC, the heat maps of achievable capacity under FCC rules (Fig. 15(a)) and Cog-TV (Fig. 15(b)) have similar patterns as their SA counter parties (Figs. 12), for achievable capacity is dependent of SA. Lognormal fading causes randomness across cells on the heat map of achievable capacity (Fig. 15(c)), which is consistent with the theoretical one (Fig. 15(b)) at Zip code level. The CDFs of achievable capacity from *micro model* (Fig. VII-C) shows that estimate of city-level capacity model is slightly (1.9% for median) lower than that w/ lognormal fading.

[3]Only the top 14-16 TV networks with available ratings data are replaced. Variation of SHRs of Top-4 Channels are up to 22.5-38%, with relative standard deviation of 11.0-16.9%.

TABLE V
PRIME TIME AVERAGE INDOOR ACHIEVABLE CAPACITY, UNIT: MBPS

Rules (rating)	d (m)	**NYC** Fixed	**NYC** Portable	**Lincoln** Fixed	**Lincoln** Portable
FCC	10	189.2	131.3	2499.8	1748.2
	20	155.6	111.1	2070.1	1478.7
Cog-TV, (Zipf SHR)	10	1255.7	1031.7	3360.7	2383.3
	20	897.8	770.2	2683.6	1944.7
Cog-TV, (Random SHR)	10	616.1	458.8	3349.7	2357.0
	20	453.5	371.7	2676.1	1927.0
Cog-TV, (Uniform SHR)	10	469.9	376.5	3347.2	2357.3
	20	353.3	291.0	2674.2	1927.3

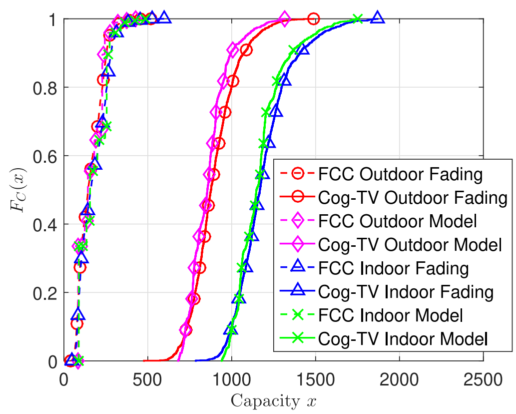

Fig. 16. CDFs of Achievable Capacity in NYC, Zipf SHR, Micro Model, ITU-R P1411, w/ and w/o Lognormal Fading, Outdoor and Indoor.

The average achievable capacity in NYC and Lincoln under FCC rules and Cog-TV framework w/ different SHRs and service radius are reported in Table V. For service radius of $d = 10$ m, Cog-TV brings NYC a 2.5-6.6-fold increase in achievable capacity for fixed TVBDs and 2.8-7.8-fold increase for portable TVBDs over FCC rules. In Lincoln, the increases are 1.34-fold for fixed and 1.36-fold portable TVBDs. Compared to TVWS, primary interference significantly lowers the session capacity on TVBS [38]. As a result, the gain of Cog-TV on achievable capacity is lower than gain on SA, especially for rural cities with abundant TVWS like Lincoln. Increase of service radius d from 10 m to 20 m can decrease the achievable capacity for about 35%. Higher path loss exponent [76] increases achievable capacity in NYC by 421 Mbps on average over the lower one [78] with all other conditions being the same [38], since interference can be better managed in environments with higher isolation between SUs and neighboring PUs. On individual TVBS channel, city-level capacity model is consistent with *micro model* [38].

E. Temporal Dynamics

The prime time (7–9 pm) results in Sections VII-B–VII-D represent the worst 1–2 hours in a day for SU. Considering the hourly HUT pattern in Fig. 1(b), the average SA in NYC under Cog-TV would increase at most by 21% and 24% for fixed and portable TVWS bands, respectively (Fig. 17(a)). However, variations of SA in Lincoln is negligible due to low TV receiver density (Fig. 17(b)). The heat maps of SA at different hours in NYC are further illustrated in [38].

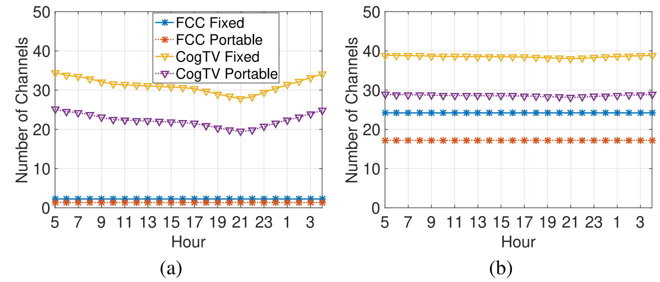

Fig. 17. Intra-Day Mean Spectrum Availability with Zipf Rating. (a) New York City. (b) Lincoln, NE.

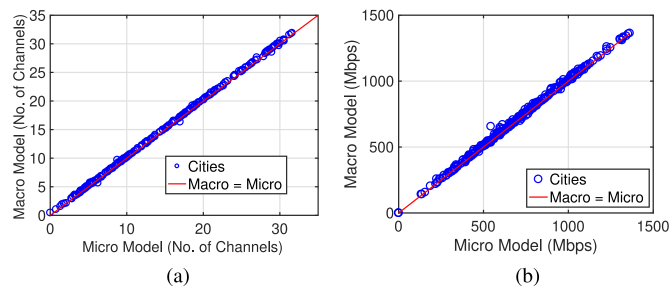

Fig. 18. Macro Model v.s. Micro Models on Estimating Performance in 274 U.S. Cities. (a) Average Black-Space Spectrum Availability. (b) Average Black-Space Achievable Capacity.

VIII. NATION-WIDE EVALUATION

Based on the approaches in Section VII, the average SA and achievable capacity of 274 major cities in the continental US are estimated. The average SA and capacity of TVBS in the 274 US cities are shown in Figs. 18(a) and 18(b), respectively, where the x, y axes are the average values of a city from *micro* and *macro models*, respectively. Compared to *micro model*, *macro model* with homogeneous TV coverage assumption, has RMS errors of 0.24 (1.18%) and 16.82 Mbps (1.37%) on average SA and achievable capacity, respectively. It shows that city-level TVBS models can get similar accuracy of geographical analysis at only 5%–10% computational cost.

The average capacity per TVBS channel, $E(C^b(c,t) \mid c \in y)/|\mathbb{B}_y|$, in portable TVBD band, decreases by the spatio-spectral average TV signal strength of a city (Fig. 19(a)). To address the primary interference, indoor operation and interference cancellation can on average increase the capacity per TVBS channel by 10.2 and 31.4 Mbps, respectively, compared to outdoors.

Finally, Cog-TV and FCC rules are compared across the 274 U.S. cities on normalized SA (Fig. 19(b)) and achievable capacity in portable TVWS band (Fig. 19(c)), where x axis is the average population density. Normalized SA of a city is defined as the average SA over the total number of channels in TVWS band w/o reserved channels. Nationally, Cog-TV can increase TV spectrum utilization efficiency to its intrinsic limit set by OTA TV receiver density, and the capacity for portable TVBD typically by 500–1000 Mbps w/ IC outdoor. In the two-tier U.S. OTA TV market [6], for cities with dense population and limited TVWS, e.g. many of the top-20 cities by population [38], Cog-TV could increase SA and capacity by multiple times.

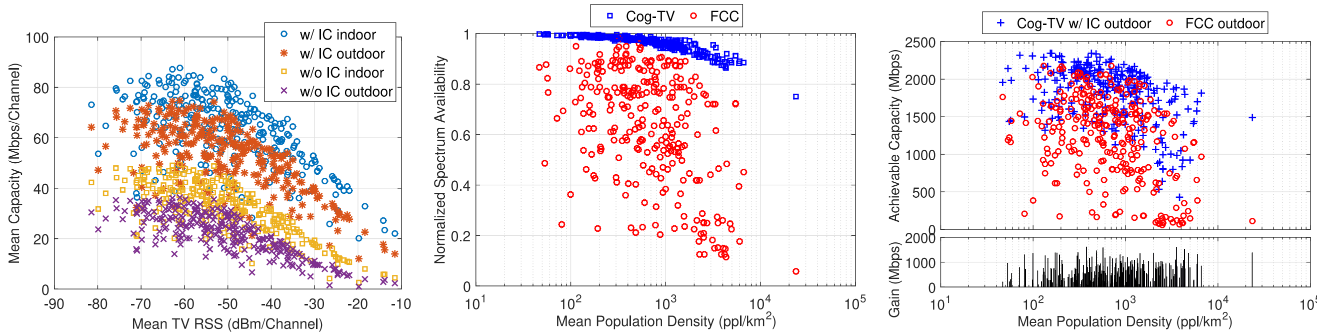

(a) (b) (c)

Fig. 19. Cog-TV framework and FCC rules in 274 Major US Cities. (a) Average Capacity Per Black Space Channel in Portable TVWS band v.s. Average TV RSS. (b) Normalized Average Spectrum Availability in TVWS band v.s. Average Population Density. (c) Average Achievable Capacity in Portable TVWS band v.s. Average Population Density.

IX. Conclusion and Future Directions

In this paper, we provide a holistic view of the availability and capacity of TV spectrum when TV viewers instead of TV broadcasters are considered as primary users. Although the analysis is still preliminary and could be refined with more secondary user traffic conditions, include other primary users (e.g. mobile TV, wireless microphone), and using TV ownership and viewership data of finer spatial granularity (may not publicly available). It demonstrates that secondary access of TV spectrum by leveraging TV receiver activities is technically feasible, and has significant potential in elevating the spectrum crisis in major urban areas.

Technically, operation in TV black spaces faces two major challenges: (I) interference from TV towers to SUs, and (II) interference from SUs to TV viewers. The first challenge can be addressed by indoor operations and/or various interference cancellation techniques, such as leveraging knowledge of TV signals [79], multi-antenna technologies [36], [80], and techniques similar to inter-cell interference cancellation in femto-cell architectures [81], [82]. Secondary network also needs protocols adaptive to the highly dynamic radio environment in black space.

The second challenge of preventing SU interference to TV viewers requires several unique features. Strict timing on SU channel evacuation is required to protect TV user experience. Specific system design and additional infrastructure might be required. Transmit power control at SU requires spectrum sensing (e.g. collaborative sensing) to estimate TV signal strength and/or radio propagation environments rather than just detect its existence. Beamforming [36] can reduce harmful interference to TV users. The biggest challenge, however, is integration of TV viewership information into spectrum management. To this end, the most effective and scalable approach would be leverage the new ATSC 3.0 standard by creating relevant specification of spectrum sharing. To serve a city or region, a high performance spectrum management infrastructure would be required in addition to current spectrum databases for real-time interaction with primary and secondary users, as well as to update the spectrum availability with much finer spatial-temporal granularity than current TVWS databases [38]. Besides technology, further discussions in policy, business, and privacy aspects are required to reach the significant potential of TV spectrum with this approach. We believe that the results in this paper will motivate such discussions.

References

[1] I. F. Akyildiz, W.-Y. Lee, M. C. Vuran, and S. Mohanty, “NeXt generation/dynamic spectrum access/cognitive radio wireless networks: A survey,” *Comput. Netw.*, vol. 50, no. 13, pp. 2127–2159, Sep. 2006.

[2] *Second Memorandum Opinion and Order*, Federal Commun. Commission, Washington, DC, USA, Sep. 2010.

[3] *Third Memorandum Opinion and Order*, Federal Commun. Commission, Washington, DC, USA, Sep. 2012.

[4] K. Harrison, S. Mishra, and A. Sahai, “How much white-space capacity is there?” in *Proc. IEEE Int. Symp. Dyn. Spectr. Access Netw.*, Apr. 2010, pp. 1–10.

[5] F. Hessar and S. Roy, “Capacity considerations for secondary networks in TV white space,” *IEEE Trans. Mobile Comput.*, vol. 14, no. 9, pp. 1780–1793, Sep. 2015.

[6] Z. Zhao and M. C. Vuran, “Population density statistics and OTA TV channel availability via Cog-TV in major United States cities,” Univ. Nebraska-Lincoln, Lincoln, NE, USA, Tech. Rep. TR-UNL-CSE-2014-0006, Dec. 2014. [Online]. Available: http://www.unl.edu

[7] S. Bhattarai, J. M. J. Park, B. Gao, K. Bian, and W. Lehr, “An overview of dynamic spectrum sharing: Ongoing initiatives, challenges, and a roadmap for future research,” *IEEE Trans. Cogn. Commun. Netw.*, vol. 2, no. 2, pp. 110–128, Jun. 2016.

[8] J. Rosen, “The future of spectrum,” Center Technol. Innov., Brookings Inst., Washington, DC, USA, Aug. 2011.

[9] *Broadcast Incentive Auction and Post-Auction Transition*, Federal Commun. Commission, Washington, DC, USA, May 2017. [Online]. Available: https://www.fcc.gov/about-fcc/fcc-initiatives/incentive-auctions

[10] “The total audience report: Q4, 2016,” Nielsen Co., New York, NY, USA, Apr. 2017.

[11] “Advertising and audiences: The state of the media,” Nielsen Co., New York, NY, USA, Apr. 2013.

[12] “HUT PUT national prime trends,” Nielsen Co., New York, NY, USA, 2015. [Online]. Available: www.tvb.org/research/measurement/4749

[13] H. Beville, *Audience Ratings: Radio, Television, and Cable*. Mahwah, NJ, USA: L. Erlbaum Associates, 1985.

[14] H. Bezabih, B. Ellingsaeter, J. Noll, and T. T. Maseng, “Digital broadcasting: Increasing the available white space spectrum using TV receiver information,” *IEEE Veh. Technol. Mag.*, vol. 7, no. 1, pp. 24–30, Mar. 2012.

[15] *Statement: Implementing TV White Spaces*, Ofcom, London, U.K., Feb. 2015.

[16] L. Shi, E. Obregon, K. won Sung, J. Zander, and J. Bostrom, “CellTV on the benefit of TV distribution over cellular networks: A case study,” *IEEE Trans. Broadcast.*, vol. 60, no. 1, pp. 73–84, Mar. 2014.

[17] S. Mishra, “Maximizing available spectrum for cognitive radios,” Ph.D. dissertation, Dept. Comput. Sci. Eng., Univ. California Berkeley, Berkeley, CA, USA, Jan. 2010.

[18] L. Fay, L. Michael, D. Gmez-Barquero, N. Ammar, and M. W. Caldwell, "An overview of the ATSC 3.0 physical layer specification," *IEEE Trans. Broadcast.*, vol. 62, no. 1, pp. 159–171, Mar. 2016.

[19] *Authorizing Permissive Use of the "Next Generation" Broadcast Television Standard*, Federal Commun. Commission, Washington, DC, USA, Nov. 2017.

[20] M. F. Ursu *et al.*, "Interactive TV narratives: Opportunities, progress, and challenges," *ACM Trans. Multimedia Comput. Commun. Appl.*, vol. 4, no. 4, pp. 1–39, Nov. 2008.

[21] *Connecting American: The National Broadband Plan*, Federal Commun. Commission, Washington, DC, USA, 2010.

[22] K. Harrison and A. Sahai, "Seeing the bigger picture: Context-aware regulations," in *Proc. IEEE Int. Symp. Dyn. Spectr. Access Netw.*, Oct. 2012, pp. 21–32.

[23] J. van de Beek, J. Riihijarvi, A. Achtzehn, and P. Mahonen, "TV white space in europe," *IEEE Trans. Mobile Comput.*, vol. 11, no. 2, pp. 178–188, Feb. 2012.

[24] "Google spectrum database: TV stations in the U.S.," Google, 2013. [Online]. Available: https://www.google.com/get/spectrumdatabase/data/

[25] M. Caleffi and A. S. Cacciapuoti, "Optimal database access for TV white space," *IEEE Trans. Commun.*, vol. 64, no. 1, pp. 83–93, Jan. 2016.

[26] M. A. McHenry *et al.*, "Chicago spectrum occupancy measurements & analysis and a long-term studies proposal," in *Proc. 1st Int. Workshop Technol. Policy Accessing Spectr.*, Boston, MA, USA, Aug. 2006.

[27] T. Taher *et al.*, "Long-term spectral occupancy findings in chicago," in *Proc. IEEE Int. Symp. Dyn. Spectr. Access Netw.*, May 2011, pp. 100–107.

[28] M. Islam *et al.*, "Spectrum survey in singapore: Occupancy measurements and analyses," in *Proc. Int. Conf. Cogn. Radio Oriented Wireless Netw. Commun.*, May 2008, pp. 1–7.

[29] S. Yin, D. Chen, Q. Zhang, M. Liu, and S. Li, "Mining spectrum usage data: A large-scale spectrum measurement study," *IEEE Trans. Mobile Comput.*, vol. 11, no. 6, pp. 1033–1046, Jun. 2012.

[30] T. X. Brown, E. Pietrosemoli, M. Zennaro, A. Bagula, H. Mauwa, and S. M. Nleya, "A survey of TV white space measurements," in *E-Infrastructure and E-Services for Developing Countries*, A. Nungu, B. Pehrson, and J. Sansa-Otim, Eds. Cham, Switzerland: Springer, 2015, pp. 164–172.

[31] X. Ying *et al.*, "Exploring indoor white spaces in metropolises," *ACM Trans. Intell. Syst. Technol.*, vol. 9, no. 1, pp. 1–25, Aug. 2017.

[32] J. Zhang, W. Zhang, M. Chen, and Z. Wang, "Winet: Indoor white space network design," in *Proc. IEEE Conf. Comput. Commun.*, Apr. 2015, pp. 630–638.

[33] X. Ying, F. Hessar, and S. Roy, "Indoor–Outdoor TV white and gray space availability: A U.S. case study," in *TV White Space Communications and Networks* (Series in Electronic and Optical Materials), R. Stewart, D. Crawford, and A. Stirling, Eds. Sawston, U.K.: Woodhead Publishing, 2018, pp. 47–71.

[34] B. Gao *et al.*, "Incentivizing spectrum sensing in database-driven dynamic spectrum sharing," in *Proc. 35th Annu. IEEE Int. Conf. Comput. Commun.*, Apr. 2016, pp. 1–9.

[35] Z. Zhao, M. C. Vuran, D. Batur, and E. Ekici, "Ratings for spectrum: Impacts of TV viewership on TV whitespace," in *Proc. IEEE Global Commun. Conf.*, Dec. 2014, pp. 941–947.

[36] X. Zhang and E. W. Knightly, "Watch: Wifi in active TV channels," in *Proc. 16th ACM Int. Symp. Mobile Ad Hoc Netw. Comput.*, New York, NY, USA, 2015, pp. 7–16.

[37] L. Zhang *et al.*, "Interference-constrained access opportunity distribution for secondary communication in TV white space," in *Proc. IEEE Wireless Commun. Netw. Conf.*, Mar. 2015, pp. 1888–1893.

[38] Z. Zhao, M. C. Vuran, D. Batur, and E. Ekici, "Technical report: Supplemental simulation and experimental results for Cog-TV," Dept. Comput. Sci. Eng., Univ. Nebraska-Lincoln, Lincoln, NE, USA, Tech. Rep. TR-UNL-CSE-2018-0002, Oct. 2018. [Online]. Available: http://www.unl.edu

[39] L. Bedogni, A. Achtzehn, M. Petrova, P. Mähönen, and L. Bononi, "Performance assessment and feasibility analysis of IEEE 802.15.4m wireless sensor networks in TV grayspaces," *ACM Trans. Sensor Netw.*, vol. 13, no. 1, pp. 1–27, Jan. 2017.

[40] Z. Zhao and M. C. Vuran, "Modeling aggregate interference with heterogeneous secondary users and passive primary users for dynamic admission and power control in TV spectrum," in *Proc. 2nd Int. Balkan Conf. Commun. Netw.*, Podgorica, Montenegro, Jun. 2018.

[41] A. Goldsmith, S. Jafar, I. Maric, and S. Srinivasa, "Breaking spectrum gridlock with cognitive radios: An information theoretic perspective," *Proc. IEEE*, vol. 97, no. 5, pp. 894–914, May 2009.

[42] I. Akyildiz, W.-Y. Lee, M. C. Vuran, and S. Mohanty, "A survey on spectrum management in cognitive radio networks," *IEEE Commun. Mag.*, vol. 46, no. 4, pp. 40–48, Apr. 2008.

[43] Y. Beyene *et al.*, "Effect of secondary transmission on primary pilot carriers in overlay cognitive radios," in *Proc. Int. Conf. Cogn. Radio Oriented Wireless Netw.*, Jul. 2013, pp. 111–116.

[44] B. Wild *et al.*, "Detecting primary receivers for cognitive radio applications," in *Proc. IEEE Int. Symp. Dyn. Spectr. Access Netw.*, Nov. 2005, pp. 124–130.

[45] D. Xue, E. Ekici, and M. C. Vuran, "Cooperative spectrum sensing in cognitive radio networks using multidimensional correlations," *IEEE Trans. Wireless Commun.*, vol. 13, no. 4, pp. 1832–1843, Apr. 2014.

[46] J. G. Webster, "Nielsen ratings," in *The International Encyclopedia of Communication*, vol. 7. Oxford, U.K.: Blackwell, 2008, pp. 3318–3320.

[47] Y. Luo, L. Gao, and J. Huang, "Spectrum reservation contract design in TV white space networks," *IEEE Trans. Cogn. Commun. Netw.*, vol. 1, no. 2, pp. 147–160, Jun. 2015.

[48] N. Miridakis and D. Vergados, "A survey on the successive interference cancellation performance for single-antenna and multiple-antenna OFDM systems," *IEEE Commun. Surveys Tut.*, vol. 15, no. 1, pp. 312–335, Firstquarter 2013.

[49] N. Liu, H. Cui, S.-H. G. Chan, Z. Chen, and Y. Zhuang, "Dissecting user behaviors for a simultaneous live and VOD IPTV system," *ACM Trans. Multimedia Comput. Commun. Appl.*, vol. 10, no. 3, pp. 1–16, Apr. 2014.

[50] E. Veloso, V. Almeida, W. Meira, A. Bestavros, and S. Jin, "A hierarchical characterization of a live streaming media workload," *IEEE/ACM Trans. Netw.*, vol. 14, no. 1, pp. 133–146, Feb. 2006.

[51] K. Sripanidkulchai, B. Maggs, and H. Zhang, "An analysis of live streaming workloads on the internet," in *Proc. 4th ACM SIGCOMM Conf. Internet Meas.*, New York, NY, USA, 2004, pp. 41–54.

[52] J. Walrand, *An Introduction to Queueing Networks*. Englewood Cliffs, NJ, USA: Prentice-Hall, 1988.

[53] H. ElSawy, E. Hossain, and M. Haenggi, "Stochastic geometry for modeling, analysis, and design of multi-tier and cognitive cellular wireless networks: A survey," *IEEE Commun. Surveys Tut.*, vol. 15, no. 3, pp. 996–1019, Thirdquarter 2013.

[54] Y. Hong, "On computing the distribution function for the poisson binomial distribution," *Comput. Statist. Data Anal.*, vol. 59, pp. 41–51, 2013.

[55] "Nielsen local TV view: Glossary," Nielsen Co., New York, NY, USA, 2014.

[56] "Weekly viewing data," Broadcasters' Audience Res. Board Ltd., London, U.K., 2014. [Online]. Available: http://www.barb.co.uk/

[57] "This weeks broadcast ratings," Media Life Magazine, Dec. 2015. [Online]. Available: http://www.medialifemagazine.com/this-weeks-broadcast-ratings/

[58] M. Cha, P. Rodriguez, J. Crowcroft, S. Moon, and X. Amatriain, "Watching television over an IP network," in *Proc. 8th ACM SIGCOMM Conf. Internet Meas.*, New York, NY, USA, 2008, pp. 71–84.

[59] T. Qiu, Z. Ge, S. Lee, J. Wang, Q. Zhao, and J. Xu, "Modeling channel popularity dynamics in a large IPTV system," in *Proc. 11th Int. Joint Conf. Meas. Model. Comput. Syst.*, New York, NY, USA, 2009, pp. 275–286.

[60] P. Evensen and H. Meling, "A paradigm comparison for collecting TV channel statistics from high-volume channel zap events," in *Proc. 5th ACM Int. Conf. Distrib. Event-Based Syst.*, New York, NY, USA, 2011, pp. 317–326.

[61] M. Newman, "Power laws, Pareto distributions and Zipf's law," *Contemporary Phys.*, vol. 46, no. 5, pp. 323–351, 2005.

[62] "U.S. homes add even more TV sets in 2010," Nielsen Co., New York, NY, USA, Apr. 2010. [Online]. Available: http://www.nielsen.com/us/en/newswire/2010/u-s-homes-add-even-more-tv-sets-in-2010.html

[63] D. Rempe *et al.*, "A cognitive radio TV prototype for effective TV spectrum sharing," in *Proc. IEEE Int. Symp. Dyn. Spectr. Access Netw.*, Mar. 2017, pp. 117–118.

[64] C. Y. Lee, C. K. Hong, and K. Y. Lee, "Reducing channel zapping time in IPTV based on user's channel selection behaviors," *IEEE Trans. Broadcast.*, vol. 56, no. 3, pp. 321–330, Sep. 2010.

[65] *Measuring Broadband America Fixed Broadband Report-2016*, Federal Commun. Commission, Washington, DC, USA, Dec. 2016.

[66] W. Hoeffding and W. Hoeffding, "A combinatorial central limit theorem," *Ann. Math. Statist.*, vol. 22, pp. 558–566, 1951.

[67] "Longley-Rice methodology for evaluating TV coverage and interference," Office Eng. Technol., Federal Commun. Commission, Washington, DC, USA, Tech. Rep. OET B 69, Feb. 2004. [Online]. Available: https://transition.fcc.gov/bureaus/oet/info/documents/bulletins/oet69/oet69.pdf

[68] "47 CFR 73.610—Minimum distance separations between stations," Code Federal Regulations (annual edition), U.S. Government Publishing Office, Washington, DC, USA, Oct. 2009. [Online]. Available: https://www.gpo.gov

[69] Receivers and Spectrum Working Group, "Interference limits policy the use of harm claim thresholds to improve the interference tolerance of wireless systems," Federal Commun. Commission, Washington, DC, USA, Feb. 2013.

[70] E. W. Weisstein, "Normal difference distribution," 2003. [Online]. Available: http://mathworld.wolfram.com/NormalDifferenceDistribution.html

[71] M. D. Springer, *The Algebra of Random Variables* (Probability and Statistics Series). Hoboken, NJ, USA: Wiley, 1979.

[72] "Census 2010 data," CENSUS, 2010. [Online]. Available: http://factfinder2.census.gov

[73] "U.S. and world population clock," CENSUS, Jul. 2016. [Online]. Available: https://www.census.gov/popclock/

[74] T. Qiu, Z. Ge, S. Lee, J. Wang, J. Xu, and Q. Zhao, "Modeling user activities in a large IPTV system," in *Proc. ACM SIGCOMM Conf. Internet Meas. Conf.*, New York, NY, USA, 2009, pp. 430–441.

[75] "Universal software radio peripheral (USRP)," Ettus Res., Santa Clara, CA, USA, 2016. [Online]. Available: https://www.ettus.com/

[76] *Propagation Data and Prediction Methods for the Planning of Short-Range Outdoor Radiocommunication Systems and Radio Local Area Networks in the Frequency Range 300 MHz to 100 GHz*, ITU-R P.1411-9, International Telecommunications Union, Geneva, Switzerland, Jun. 2017.

[77] *FM and TV Propagation Curves*, FCC Encyclopedia, Federal Commun. Commission, Washington, DC, USA, Oct. 2011.

[78] W. Daniel and H. Wong, "Propagation in suburban areas at distances less than ten miles," Office Eng. Technol., Federal Commun. Commission, Washington, DC, USA, Tech. Rep. OET TM 91-1, Jan. 1991. [Online]. Available: https://www.fcc.gov/oet/info/documents/technical/tm91-1.pdf

[79] S. Zhang, S.-C. Liew, and H. Wang, "Blind known interference cancellation," *IEEE J. Sel. Areas Commun.*, vol. 31, no. 8, pp. 1572–1582, Aug. 2013.

[80] N. Anand *et al.*, "The case for UHF-band MU-MIMO," in *Proc. 20th Annu. Int. Conf. Mobile Comput. Netw.*, 2014, pp. 29–40.

[81] I. F. Akyildiz, D. M. Gutierrez-Estevez, R. Balakrishnan, and E. Chavarria-Reyes, "LTE-Advanced and the evolution to beyond 4G (B4G) systems," *Phys. Commun.*, vol. 10, pp. 31–60, 2014.

[82] J. Andrews, H. Claussen, M. Dohler, S. Rangan, and M. Reed, "Femtocells: Past, present, and future," *IEEE J. Sel. Areas Commun.*, vol. 30, no. 3, pp. 497–508, Apr. 2012.

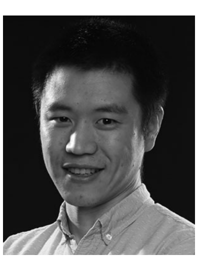

Zhongyuan Zhao (S'13–M'18) received the B.Sc. and M.S. degrees in electronic and electrical engineering from the University of Electronic Science and Technology of China, Chengdu, China, in 2006 and 2009, respectively. Currently, he is working toward the Ph.D. degree in computer engineering with the University of Nebraska-Lincoln, Lincoln, NE, USA, under the guidance of Prof. M. C. Vuran. From 2009 to 2011, he was with ArrayComm LLC., as a Digital Signal Processing Software Engineer, and from 2011 to 2013, he was with Ericsson (China) Communications Co. Ltd., as an Integration and Verification Engineer. His current research interests include dynamic spectrum access, wireless physical layer, machine learning, and decision science. He was the recipient of the national first prize in National Undergraduate Electronic Design Contest of China in 2005, and two patents in 2012 and 2016, respectively.

Mehmet C. Vuran (S'98–M'07) received the B.Sc. degree in electrical and electronics engineering from Bilkent University, Ankara, Turkey, in 2002, and the M.S. and Ph.D. degrees in electrical and computer engineering from the Georgia Institute of Technology, Atlanta, GA, USA, in 2004 and 2007, respectively, under the guidance of Prof. I. F. Akyildiz. Currently, he is a Susan J. Rosowski Associate Professor with the Department of Computer Science and Engineering, the University of Nebraska-Lincoln, Lincoln, NE, USA, and Robert B. Daugherty Water for Food Institute Fellow. He is the co-author of *Wireless Sensor Networks* textbook. His current research interests include dynamic spectrum access, wireless underground communications, agricultural Internet of Things, wearable embedded systems, and connected autonomous systems. He is an Associate Editor for the IEEE TRANSACTIONS ON WIRELESS COMMUNICATIONS, the *Computer Networks Journal* (Elsevier), and the IEEE COMMUNICATIONS SURVEYS AND TUTORIALS. He was recognized as a highly cited researcher three years in a row, in 2014, 2015, and 2016, by Thomson Reuters in recognition of ranking among the top 1% of researchers for most cited documents in Computer Science. He is the recipient of an NSF CAREER award in 2010.

Demet Batur received the B.S. degree in industrial engineering from Marmara University, Istanbul, Turkey, in 2001, and the M.S. and Ph.D. degrees in industrial and systems engineering from the Georgia Institute of Technology, Atlanta, GA, USA, in 2003 and 2006, respectively. Currently, she is an Assistant Professor with the Department of Supply Chain Management and Analytics, College of Business, the University of Nebraska-Lincoln, Lincoln, NE, USA. Her current research interests include operations management, decision science, supply chain integration and management, and systems simulation and analysis.

Eylem Ekici (S'99–M'02–SM'11–F'17) received the B.S. and M.S. degrees in computer engineering from Bogazici University, Istanbul, Turkey, in 1997 and 1998, respectively, and the Ph.D. degree in electrical and computer engineering from the Georgia Institute of Technology, Atlanta, GA, USA, in 2002. Currently, he is a Professor with the Department of Electrical and Computer Engineering, The Ohio State University, Columbus, OH, USA. His current research interests include dynamic spectrum access, vehicular communication systems, and next generation wireless systems, with a focus on algorithm design and resource management. He is a member of the ACM. He was the general Co-Chair of ACM MobiCom 2012. He was also the TPC Co-Chair of the IEEE INFOCOM 2017. He is an Associate Editor-in-Chief for the IEEE TRANSACTIONS ON MOBILE COMPUTING, and a former Associate Editor for the IEEE/ACM TRANSACTIONS ON NETWORKING, the IEEE TRANSACTIONS ON MOBILE COMPUTING, and the *Computer Networks Journal* (Elsevier).